European Journal of Medicinal Chemistry 224 (2021) 113673

Contents lists available at ScienceDirect

European Journal of Medicinal Chemistry

journal homepage: http://www.elsevier.com/locate/ejmech

Design and synthesis of novel orally selective and type II pan-TRK inhibitors to overcome mutations by property-driven optimization

Mu-Chun Li [a, b, c], Wen-Hsing Lin [a], Pei-Chen Wang [a, 1], Yu-Chieh Su [a, 1], Pei-Yi Chen [a], Chu-Min Fan [a], Ching-Ping Chen [a], Chen-Lung Huang [a], Chun-Hsien Chiu [a], Ling Chang [a], Chiung-Tong Chen [a], Teng-Kuang Yeh [a], Hsing-Pang Hsieh [a, b, c, *]

[a] Institute of Biotechnology and Pharmaceutical Research, National Health Research Institutes, No. 35, Keyan Road, Zhunan Town, Miaoli County, 350401, Taiwan, ROC
[b] Department of Chemistry, National Tsing Hua University, No. 101, Sec. 2, Kuang-Fu Road, Hsinchu, 300044, Taiwan, ROC
[c] Biomedical Translation Research Center, Academia Sinica, No. 99, Ln. 130, Sec. 1, Academia Road, Taipei City, 115202, Taiwan, ROC

ARTICLE INFO

Article history:
Received 12 May 2021
Received in revised form
22 June 2021
Accepted 24 June 2021
Available online 29 June 2021

Keywords:
Tropomyosin receptor kinase (TRK)
Kinase inhibitor
Fusion
Mutation
Property-driven optimization

ABSTRACT

Rare oncogenic NTRK gene fusions result in uncontrolled TRK signaling leading to various adult and pediatric solid tumors. Based on the architecture of our multi-targeted clinical candidate **BPR1K871** (**10**), we designed and synthesized a series of quinazoline compounds as selective and orally bioavailable type II TRK inhibitors. Property-driven and lead optimization strategies informed by structure-activity relationship studies led to the identification of **39**, which showed higher (about 15-fold) selectivity for TRKA over AURA and AURB, as well as potent cellular activity (IC_{50} = 56.4 nM) against the KM12 human colorectal cancer cell line. **39** also displayed good AUC and oral bioavailability (F = 27%), excellent *in vivo* efficacy (TGI = 64%) in a KM12 xenograft model, and broad-spectrum *anti*-TRK mutant potency (IC_{50} = 3.74–151.4 nM), especially in the double-mutant TRKA enzymatic assays. **39** is therefore proposed for further development as a next-generation, selective, and orally-administered type II TRK inhibitor.

1. Introduction

In the tropomyosin receptor kinase (TRK) family, TRKA, TRKB, and TRKC are the members of tyrosine receptor kinase encoded by the NTRK1, NTRK2, and NTRK3 genes, respectively. These tyrosine kinases are highly expressed in neuronal tissues and play crucial roles in the development and function of neurons by neurotrophin (NT) activation [1]. The corresponding neurotrophins of TRK kinases include nerve growth factor (NGF) for TRKA, both brain-derived growth factor and neurotrophin 4 (NT4) for TRKB, and neurotrophin 3 (NT3) for TRKC [2]. Thus, TRK kinases are involved in the regulation of synaptic strength and plasticity in the mammalian nervous system [3]. A variety of NTRK gene alterations have been diagnosed in various tumor types [4], including gene fusion, such as TPM3-NTRK1 fusion gene found in a colorectal cancer (CRC) patient in 1982 (the first NTRK gene abnormality to be identified [5]); and mutant TRKA or TRKB proteins (i.e. $TRKA^{R577G}$ and $TRKB^{P507L}$), NTRK1 deletion, and overexpressed TRK proteins have been observed in lung adenocarcinoma, melanoma, acute myeloid leukemia, neuroblastoma, etc. in the last decade [6–11]. NTRK gene fusions occur when a NTRK gene becomes abnormally connected to another unrelated gene, such as ETV6, LMNA, TPM3, etc. [12], causing uncontrolled TRK signaling leading to various adult and pediatric solid tumors. NTRK-fusions are rare (< 1%) in common cancer types but common (up to > 90%) in rare cancer types [13], and therefore the discovery of TRK inhibitors is an important therapeutic strategy.

Several TRK inhibitors have been evaluated for the treatment of a variety of cancers (Fig. 1) [14,15] including larotrectinib (Vitrakvi®, **1**) [16] and entrectinib (Rozlytrek®, **2**) [17] which were approved by U.S. Food and Drug Administration (FDA) as tumor-agnostic cancer treatment in 2018 and 2019, respectively. Larotrectinib (**1**) and entrectinib (**2**) are both proved as type I TRK inhibitors according to their binding modes with TRKA protein, in which the compounds occupy the ATP-binding site and present the "DFG-in"

* Corresponding author. Institute of Biotechnology and Pharmaceutical Research, National Health Research Institutes, No. 35, Keyan Road, Zhunan Town, Miaoli County, 350401, Taiwan, ROC.
E-mail addresses: hphshieh@nhri.edu.tw, alexhsieh@gate.sinica.edu.tw (H.-P. Hsieh).
[1] These authors contributed equally.

https://doi.org/10.1016/j.ejmech.2021.113673
0223-5234/

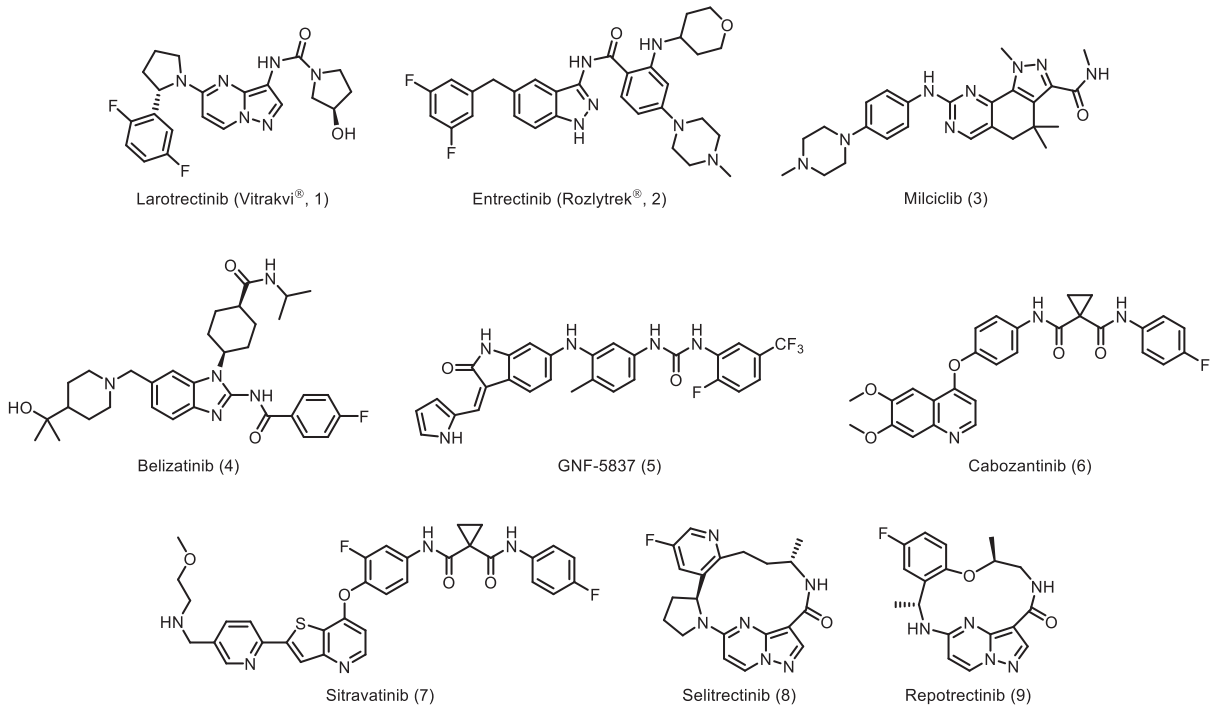

Fig. 1. Chemical structures of representative TRK inhibitors.

conformation [14]. The kinase activity is regulated by the Asp-Phe-Gly (DFG) motif significantly. Milciclib (**3**) [18] and belizatinib (**4**) [19] are two other potent type I TRK inhibitors, though neither has been approved for clinical use. Type II TRK inhibitors include GNF-5837 (**5**) [20], cabozantinib (**6**) [21], sitravatinib (**7**) [22], etc., all of which exhibit potent inhibitory activity against TRK kinases possessing "DFG-out" conformation, and some of which are under clinical investigation for the treatment of NTRK-fusion cancers. Apart from these abovementioned clinical candidates, there are numerous developing compounds under various clinical trials at different stages in the past ten years [23–25].

Despite the success of these *anti*-TRK drugs as tumor-agnostic treatment, acquired drug resistance mediated by somatic mutations in the TRK fusion is inevitable [26]. For example, the mutations $TRKA^{G595R}$ and $TRKA^{G667C}$ significantly reduce the binding affinity of larotrectinib (**1**) [27]. $TRKA^{G595R}$ is located in the solvent front region of the kinase domain, whereas $TRKA^{G667C}$ is in the xDFG position [28]. Several second-generation TRK inhibitors are in development to address these specific mutations, such as selitrectinib (LOXO-195, **8**) [29] and repotrectinib (TPX-0005, **9**) [30], whose macrocyclic structures artfully mitigate the influence of the mutant amino acids (Fig. 1). However, in clinical trials, some patients who acquired the TRKA solvent front mutation and were treated with the abovementioned compounds eventually became non-responsive, due to mutations at the xDFG position,[31] which may diminish the type I binding affinity of second-generation TRK inhibitors. Consequently, the discovery of novel selective type II TRK inhibitors to overcome the resistance is extremely important for patients who are suffering from rare cancers harboring NTRK-fusion genes. Interestingly, cabozantinib (**6**) and other type II kinase inhibitors preferentially bind to suppress xDFG TRK mutations, and showed strong inhibitory ability against double mutants in both *in vitro* and *in vivo* models [32].

Previously, we developed **BPR1K871** (**10**) [33], a multi-kinase inhibitor (MKI) for which IND approval was obtained for the treatment of solid tumors. In a kinase profiling study, **BPR1K871** (**10**) exhibited potent inhibitory activity against TRK kinases with IC_{50} values of 2.23 nM, 1.78 nM and 0.21 nM for TRKA/B/C, respectively (Fig. 2); and 6 and 13 nM against aurora kinases A (AURA) and B (AURB). However, the poor selectivity of **BPR1K871** (**10**) may cause unwanted side effects [34]; and several AURA/B inhibitors are known to be associated with common adverse effects including febrile neutropenia, stomatitis, hematological toxicities, etc. [35,36] In addition, the low oral absorption of **BPR1K871** (**10**) necessitated its intravenous administration, and raised questions regarding how frequently the patient would have to be dosed. In this study, inspired by the architecture of **BPR1K871** (**10**), we designed and synthesized a series of novel TRK inhibitors displaying excellent selectivity, significantly improved oral bioavailability, and double-digit nanomolar potency against a panel of TRK family enzymes, including some drug-resistant mutants. Structure-activity relationship (SAR) studies were accomplished using the TRKA enzymatic assay and KM12 human CRC cell line, which expresses the chimeric TPM3-TRKA protein and is hypersensitive to TRKA kinase inhibition. In addition, our novel inhibitors were counter-screened against AURA and AURB kinases, to assess their selectivity.

2. Design and chemistry

Our previous efforts to develop dual AURA and FLT3 inhibitors resulted in the identification of **BPR1K871** (**10**), a promising candidate for multiple cancer treatments (Fig. 2). However, its bioavailability was poor – perhaps due to its relatively large number of free rotatable bonds (NRB) and/or flexible dimethylaminopropoxy side chain on the quinazoline scaffold. **BPR1K871** (**10**) did incorporate a thiazole moiety on the ethylene linker, a common structural characteristic of small-molecule drugs that might be key to the poor selectivity of **BPR1K871** (**10**) [37]. To discover desired TRK inhibitors inspired by **BPR1K871** (**10**) based on property-driven strategies, we initially screened different side chains on the quinazoline scaffold, and compared the inhibitory

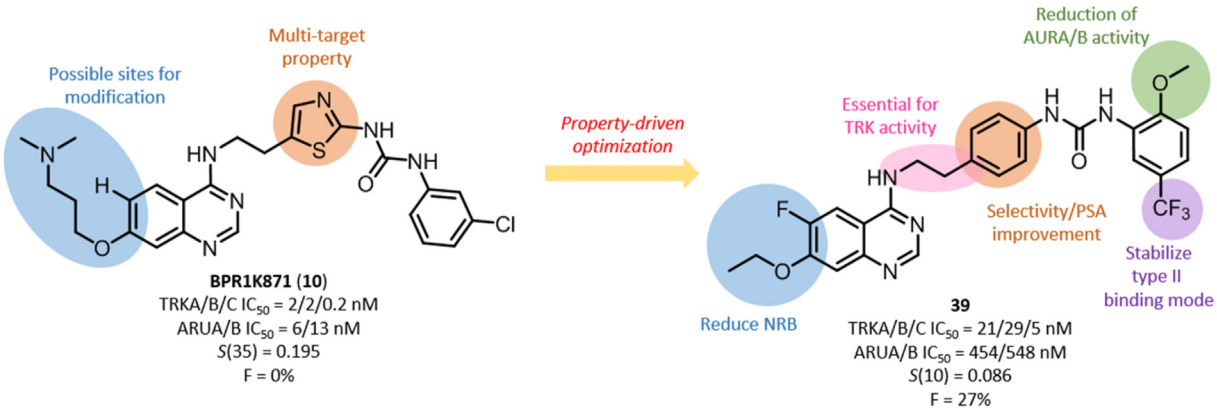

Fig. 2. Design strategy to improve the oral bioavailability and selectivity of **BPR1K871** (**10**).

activity of analogues incorporating either an ethylene thiazole or ethylene benzene linker. We also experimented with shorter linkers, to reduce the flexibility of the compounds. A selection of derivatives incorporating various functional groups were also synthesized, to screen for their effect on both TRKA and ARUA inhibitory ability.

Our synthesis started with quinazolines **11a**–**f**, to which were attached an ethylene thiazole ring (to give **12a**–**d**) or an ethylene benzene ring group (to give **19a**–**f**), respectively, as depicted in Schemes 1 and 2. The core skeletons, 4-chloroquinazoline derivatives **11a**–**f**, were either commercially available or prepared based on our previous reports [33,38]. For the ureas **14**–**17**, 4-chloroquinazoline derivatives **11a**–**d** were treated with *tert*-butyl [5-(2-aminoethyl)-1,3-thiazol-2-yl]carbamate under basic conditions to give **12a**–**d**. Then the acid-deprotected products **13a**–**d** was treated with either phenyl isocyanate or 3-chlorophenyl isocyanate to yield the target ureas **14**–**17**. Finally, the chloride moiety of **14** was substituted by *N*,*N*-dimethylamino group to obtain urea **18**.

Compounds incorporating an ethylene benzene linker were analogously synthesized. The core skeleton 4-chloroquinazoline derivatives **11a**–**f** were reacted with 4-(2-aminoethyl)aniline, 4-(aminomethyl)aniline, or benzene-1,4-diamine and trimethylamine in *N*,*N*-dimethylformamide solution to give **19a**–**f**. Then, the amine derivatives **19a**–**f** were coupled with appropriate isocyanates to give ureas **20**–**23** and **25**–**40**, respectively.

3. Results and discussion

3.1. Biological evaluation of AURA and TRKA and SAR analysis

Our initial results are presented in Table 1. Based on our knowledge and experience [39], number of rotatable bonds (NRB) and value of polar surface area (PSA) were hypothesized to influence the proportion to oral absorption, for each compound. Therefore, to improve the oral bioavailability of **BPR1K871** (**10**), several analogues bearing shorter side chains on the C-6 or C-7 positions of the quinazoline scaffold were screened. Varying the R^1

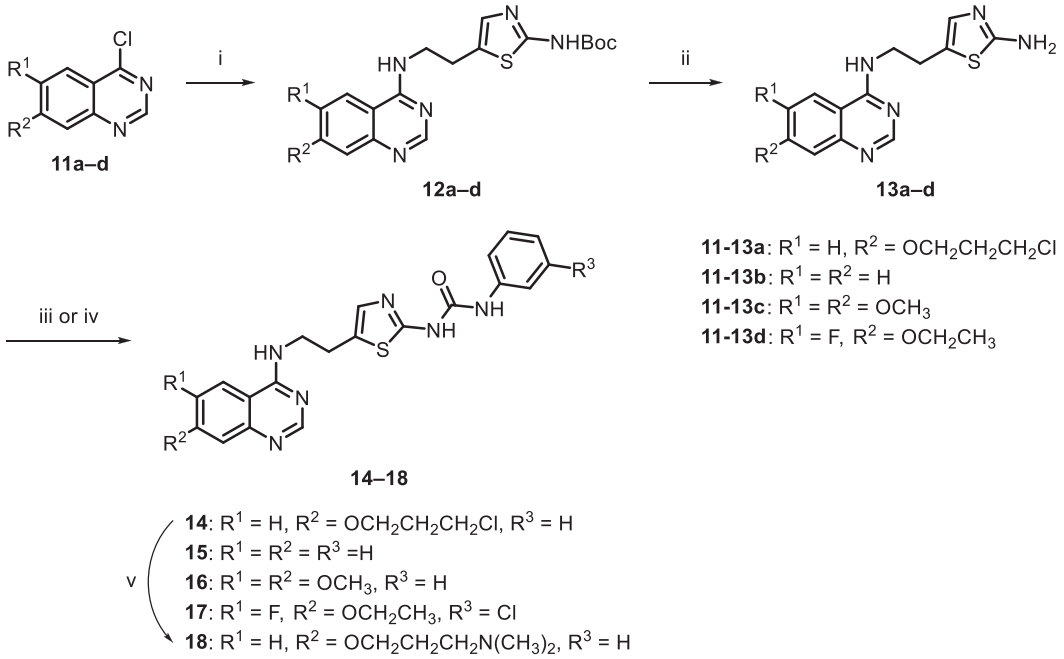

Scheme 1. Synthesis of analogues **15**–**18**.
Reagents and conditions: (i) *tert*-butyl [5-(2-aminoethyl)-1,3-thiazol-2-yl]carbamate, Et_3N, EtOH, reflux, 15 h; (ii) 6.0 N $HCl_{(aq)}$, rt, 10 h or TFA, CH_2Cl_2, rt, 12 h; (iii) PhNCO, MeOH, CH_2Cl_2, rt, 16 h; (iv) 3-Cl-PhNCO, MeOH, CH_2Cl_2, rt, 16 h; (v) *N*,*N*-dimethylamine, DMF, 100 °C, 6 h.

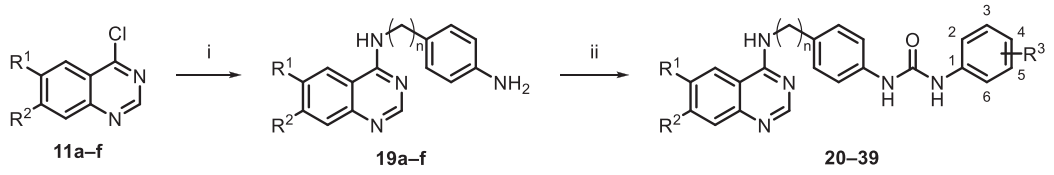

11a: R^1 = H, R^2 = $OCH_2CH_2CH_2Cl$
11b: R^1 = R^2 = H
11c: R^1 = R^2 = OCH_3
11d: R^1 = F, R^2 = OCH_2CH_3
11e: R^1 = R^2 = F
11f: R^1 = OCH_2CH_3, R^2 = F

19a: R^1 = H, R^2 = $OCH_2CH_2CH_2Cl$, n = 2
19b: R^1 = R^2 = H, n = 2
19c: R^1 = R^2 = OCH_3, n = 2
19d: R^1 = F, R^2 = OCH_2CH_3, n = 2
19d': R^1 = F, R^2 = OCH_2CH_3, n = 1
19d'': R^1 = F, R^2 = OCH_2CH_3, n = 0
19e: R^1 = R^2 = F, n = 2
19f: R^1 = OCH_2CH_3, R^2 = F, n = 2

20: R^1 = H, R^2 = $OCH_2CH_2CH_2Cl$, R^3 = H, n = 2
21: R^1 = R^2 = R^3 = H, n = 2
22: R^1 = R^2 = OCH_3, R^3 = H, n = 2
23: R^1 = F, R^2 = OCH_2CH_3, R^3 = 3-Cl, n = 2
24: R^1 = H, R^2 = $OCH_2CH_2CH_2N(CH_3)_2$, R^3 = H, n = 2
25: R^1 = F, R^2 = OCH_2CH_3, R^3 = H, n = 1
26: R^1 = F, R^2 = OCH_2CH_3, R^3 = 3-Cl, n = 1
27: R^1 = F, R^2 = OCH_2CH_3, R^3 = H, n = 0
28: R^1 = F, R^2 = OCH_2CH_3, R^3 = 3-Cl, n = 0
29: R^1 = R^2 = F, R^3 = H, n = 2
30: R^1 = R^2 = F, R^3 = 3-Cl, n = 2
31: R^1 = OCH_2CH_3, R^2 = F, R^3 = H, n = 2
32: R^1 = OCH_2CH_3, R^2 = F, R^3 = 3-Cl, n = 2
33: R^1 = F, R^2 = OCH_2CH_3, R^3 = H, n = 2
34: R^1 = F, R^2 = OCH_2CH_3, R^3 = 3-F, n = 2
35: R^1 = F, R^2 = OCH_2CH_3, R^3 = 3-CF_3, n = 2
36: R^1 = F, R^2 = OCH_2CH_3, R^3 = 3-Cl, 4-F, n = 2
37: R^1 = F, R^2 = OCH_2CH_3, R^3 = 3-CF_3, 4-Cl, n = 2
38: R^1 = F, R^2 = OCH_2CH_3, R^3 = 3-Cl, 6-OCH_3, n = 2
39: R^1 = F, R^2 = OCH_2CH_3, R^3 = 3-CF_3, 6-OCH_3, n = 2

Scheme 2. Synthesis of TRK analogues **20**–**39**.
Reagents and conditions: (i) (a) 4-(2-aminoethyl) aniline, ^{n}BuOH, reflux, 1 h; or (b) 4-(2-aminoethyl)aniline, EtOH, Et_3N, reflux, 1 h; or (c) 4-(aminomethyl)aniline, EtOH, reflux, 12 h; or (d) benzene-1,4-diamine, propan-2-ol, reflux, 1 h; (ii) R^3-PhNCO, MeOH, CH_2Cl_2, rt, 1–16 h; (iii) *N*,*N*-dimethylamine, DMF, 120 °C, 100 min, MW.

Table 1
SAR investigation by side chain modification.[a]

Compound	R^1	R^2	R^3	Ring[b]	AURA	AURB	TRKA		NRB	PSA
					IC_{50} (nM)	Inhibition @ 0.5 μM	Inhibition @ 10 μM	Inhibition @ 1 μM		
BPR1K871 (10)	H	$O(CH_2)_3N(CH_3)_2$	3-Cl	T	5.6	13[c]	100%	99%	11	132.54
15	H	H	H	T	11.1	85%	71%	1%	6	120.07
16	OCH_3	OCH_3	H	T	10.0	86%	98%	80%	8	138.53
17	F	OCH_2CH_3	3-Cl	T	8.4	64%	98%	96%	8	129.29
18	H	$O(CH_2)_3N(CH_3)_2$	H	T	6.0	76%	99%	95%	11	132.54
21	H	H	H	B	140.0	85%	18%	1%	6	78.94
22	OCH_3	OCH_3	H	B	23.0	81%	65%	6%	8	97.40
23	F	OCH_2CH_3	3-Cl	B	26.9	75%	62%	51%	8	88.17
24	H	$O(CH_2)_3N(CH_3)_2$	H	B	59.0	77%	91%	3%	11	91.41

[a] The IC_{50} and inhibition values of AURA, AURB and TRKA were performed using in-house Kinase-Glo® assay; all data are expressed as the mean of at least two independent experiments and are mostly within 15% error margins.
[b] The "T" represents a thiazole ring, and the "B" represents a benzene ring.
[c] IC_{50} value.

and R^2 substituents of **15**–**17** not only conserved the AURA, AURB and TRKA activities but also decreased the number of rotatable bonds. Next, replacement of the thiazole ring of ureas **15**–**18** with a benzene ring gave ureas **21**–**24** which had lower PSA values and AURA activities by 2.3- to 12.7-fold (Table 1). Compared with thiazole-containing analogue **17**, benzene-containing analogue **23** exhibited improved selectivity when profiled using the KINOME*scan*™ technology against a panel of 456 kinases at a concentration of 100 nM (Fig. 3, Table S1, Table S2). Taken together, **23** not only showed lower values of NRB and PSA but also satisfied selectivity than **17**, which increases the potential to obtain selective and orally efficacious compounds. These results convinced us to further study the series of compounds incorporating a benzene ring in the joint linker moiety, between the scaffold and pharmacophore.

Of urea derivatives **21**–**24** (all of which incorporated a benzene ring in the linker), **21** without any substituents on the quinazoline scaffold and a terminal phenyl ring showed the weakest TRKA ability. Urea **24** incorporating a solubilizing dimethylaminopropoxy moiety at the C-7 position was a more potent inhibitor of TRKA kinase than **21** at a concentration of 10 μM. However, the accompanying increases in both flexibility and AURA kinase inhibition were undesirable. Introduction of electron-donating methoxy groups onto both the C-6 and C-7 position of **21** to yield **22** [40] improved the TRKA inhibitory ability by a factor of approximately three times at a concentration of 10 μM; **22** was also a more potent

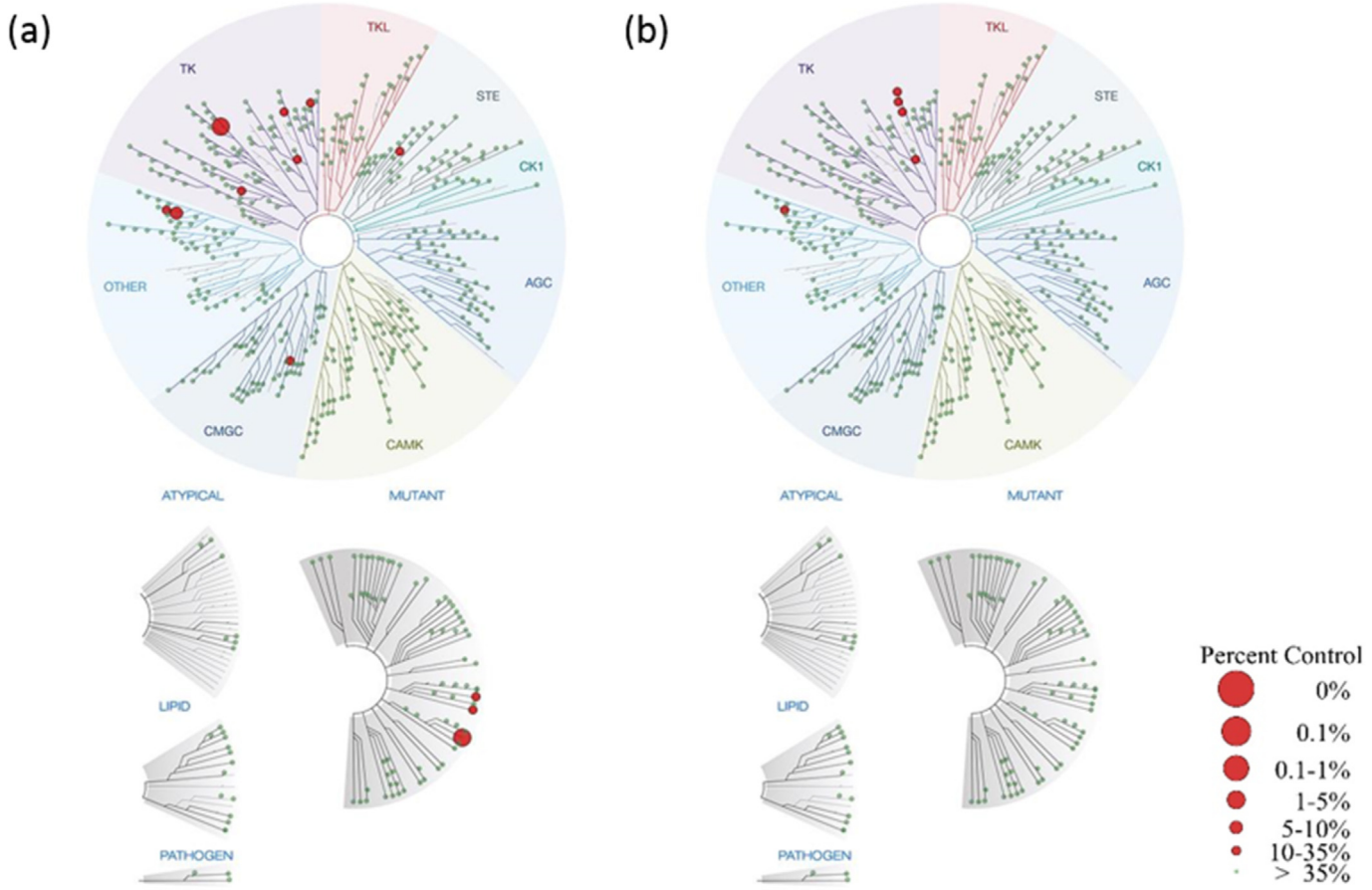

Fig. 3. Kinase profiling of **17** and **23** using KINOME*scan*™ technology. The *S*(35) of **17** and **23** were 0.022 and 0.012, respectively.

inhibitor of AURA, compared to **21**. However, of ureas **21**–**24**, **23** was the most potent inhibitor of TRKA, exhibiting 51% inhibition at a concentration of 1 μM, and having moderate AURA and AURB kinase activities. Additionally, the NRB and PSA were both relatively low. Consequently, compound **23** was regarded as the potential hit compound and selected for further studies.

3.2. Binding mode analysis of BPR1K871 (10) and 23

Molecular docking studies were undertaken to better understand the structural basis for the differences in the inhibitory potencies of **BPR1K871** (**10**) and **23** against AURA and TRKA kinases. The X-ray co-crystal structure of **BPR1K871**-AURA complex (protein data bank (PDB): 4JBO) was utilized as the basis for the study of hit compound **23** with AURA kinase. As depicted in Fig. 4a, both **BPR1K871** (**10**) and hit **23** adopt a type II binding mode with ARUA; both compounds overlap extensively in the ATP binding site. **BPR1K871** (**10**) formed seven hydrogen bond interactions with Arg137, Lys162, Glu181 and Ala213 *via* either nitrogen or oxygen atoms. The unique hydrogen bond interaction between the sulfur of the thiazole ring of **BPR1K871** (**10**) and the Asp274 backbone amide NH of the DFG motif, as well as the crucial π-π interaction between the terminal phenyl ring of **BPR1K871** (**10**) and the Phe144 in the AURA back pocket could account for the nanomolar-potency of **BPR1K871** (**10**) against AURA kinase. However, urea **23** which incorporates a benzene ring instead of a thiazole ring cannot form the specific hydrogen bond interaction with the sulfur. Additionally, the terminal phenyl ring of **23** is flipped relative to its orientation in **BPR1K871** (**10**) such that **23** is lacking the π-π interaction as well. These observations could account for the decreased AURA inhibitory ability of **BPR1K871** (**10**) compared to hit compound **23**.

Both **BPR1K871** (**10**) and hit **23** anchor to the ATP-binding site of TRKA kinase (PDB: 6PL1) [41] *via* hinge binding with Met592, adopting a type II binding mode with TRKA (Fig. 4b). The urea moiety in these two compounds generates a strong hydrogen bond interaction with the Asp668 backbone amide NH of the DFG motif, and bidentate hydrogen bonds with the Glu560 sidechain carboxylate of the α-helix. Also, the thiazole ring of **BPR1K871** (**10**) and the benzene ring of urea **23** both form the crucial π-π interaction with the Phe669 of the DFG motif, as well as the Phe589 of the gatekeeper, leading to the DFG-out conformation. Due to its strong interactions with TRKA kinase, **23** was selected for further hit-to-lead optimization.

3.3. Biological evaluation of TRKA and SAR analysis

Knowing the binding modes between hit **23** and the AURA kinase, we attempted to decreased inhibition of AURA by **23** by redesigning the ethylene linker connecting the quinazoline scaffold of **23** with the benzene ring. We hypothesized that shortening the linker might decrease binding activity with AURA/AURB by reducing the number of possible degrees of freedom – thereby impeding its interaction with the back pocket. As shown in Table 2, ureas **25** and **26** incorporating a methylene linker (n = 1) had very low TRKA and AURA/AURB inhibiting activities, as did ureas **27** and **28** (lacking a linker entirely, n = 0). The importance of the ethylene

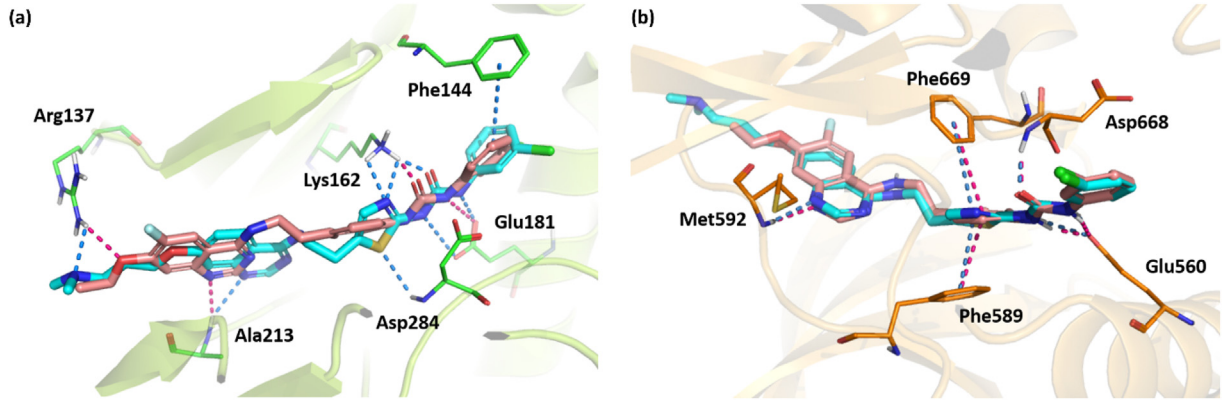

Fig. 4. Characterization of inhibitor-binding modes: (a) Binding site analysis for **BPR1K871** (**10**, cyan) and hit **23** (rose-pink) docking with AURA X-ray protein (PDB: 4JBO, green); (b) Binding site analysis for **BPR1K871** (**10**, cyan) and hit **23** (rose-pink) docking with TRKA X-ray protein (PDB: 6PL1, orange).

Table 2
In Vitro TRKA kinase inhibitory activities of inhibitors **23**–**34**.[a]

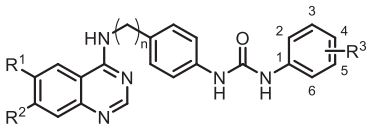

Compound	n	R^1	R^2	R^3	TRKA			KM12	AURA	AURB
					Inhibition @ 10 μM	Inhibition @ 1 μM	IC_{50} (nM)	IC_{50} (nM)	IC_{50} (nM)	Inhibition @ 0.5 μM
23	2	F	OCH_2CH_3	3-Cl	61.6%	50.7%	91.4	86.6	26.9	75%
25	1	F	OCH_2CH_3	H	14.7%	3.1%	N.D.	>10000	8%[a]	2%
26	1	F	OCH_2CH_3	3-Cl	18.6%	3.1%	N.D.	>10000	2%[a]	0%
27	0	F	OCH_2CH_3	H	23.1%	1.5%	N.D.	2400	337.8	73%
28	0	F	OCH_2CH_3	3-Cl	30.2%	7.6%	7410	1270	155.7	76%
29	2	F	F	H	17.6%	−0.2%	N.D.	2022	N.D.	75%
30	2	F	F	3-Cl	46.1%	0.7%	3590	283.3	N.D.	75%
31	2	OCH_2CH_3	F	H	21.1%	4.4%	N.D.	1523	65.6	50%
32	2	OCH_2CH_3	F	3-Cl	68.3%	15.3%	611	492.7	107.8	66%
33	2	F	OCH_2CH_3	H	7.9%	0.5%	>9000	323.7	29.2	101%
BPR1K871 (**10**)					100%	99%	36.8	42.0	6.0	75%

[a] The IC_{50} values of AURA and inhibition values of TRKA and AURB were performed using in-house Kinase-Glo® assay; the IC_{50} values of TRKA were performed using HotSpot™ kinase assay according to the manufacturer's instructions [42]; all data are expressed as the mean of at least two independent experiments and are mostly within 15% error margins.

linker was also evident in a docking study of **23**, **26** and **28**. The distance between hinge Met592 and *N*1 on the quinazoline scaffold increased with decreasing linker length (Fig. 5). Accordingly, the ethylene linker (n = 2) was concluded to be essential for TRKA activity, and was conserved in further investigations.

Next, we further explored the influence of the substituents on the quinazoline scaffold. Replacing an electron-donating group with an electron-withdrawing group at the R^2 position (for example **23** to **30**, and **33** to **29**) resulted in loss of TRKA inhibitory activity. In addition, **31** and **32** – both substituent-swapped analogues of **23** – showed weaker inhibition in the TRKA enzymatic and KM12 cellular assays. These results indicated that inhibition of TRKA and KM12 cells may be influenced by the electronic characteristics of the inhibitor. We also verified the importance of the substituent on the terminal phenyl ring. Urea analogues bearing a chloro-substituent (*cf*. **23**, **30**, **32**) were more potent inhibitors of KM12 cells than their unsubstituted counterparts (*cf*. **33**, **29**, **31**) by approximately 3–8-fold. Thus, the substituent on the distal phenyl ring was concluded to exhibit an inhibitory effect.

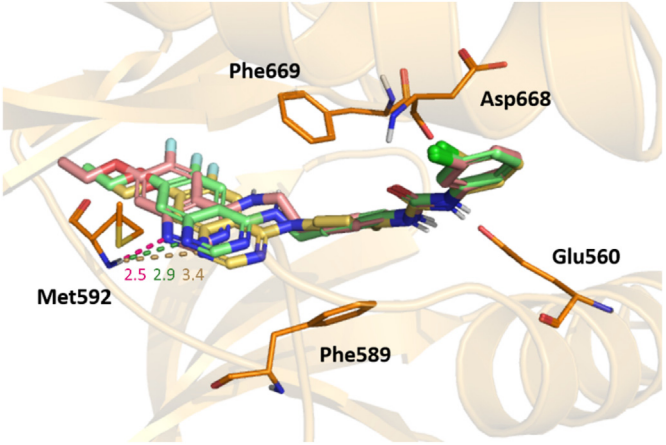

Fig. 5. Binding site analysis for hit **23** (pink), **26** (green) and **28** (yellow) docking with TRKA X-ray protein (PDB: 6PL1, orange).

The effect of the substituent at the R^3 position is outlined in Table 3. When the 3-chloro substituent was replaced by a hydrogen or fluoro group to give **33** and **34**, inhibition of TRKA and KM12 cells significantly decreased. Interestingly, **35** bearing a trifluoromethyl moiety exhibited a significantly enhanced IC_{50} value as compared to **33** and **34**. Moreover, compound **35** was 2.5-fold less effective against AURA than hit **23**. Next, we further examined the effect of di-substituted functional groups on the terminal phenyl ring. Incorporation of a phenyl ring bearing two election-withdrawing substituents (**36** (3-Cl, 4-F) and **37** (3-CF_3, 4-Cl)) decreased inhibitory TRKA potency. Based on our preceding docking studies [43], the back pocket of AURA is cramped and unable to accommodate too large of an *ortho*-substituent. Therefore, we artfully introduced a methoxyl group into **23** (to give **38**) and **35** (to give **39**), in order to exclude the undesired AURA activity. The results revealed that both **38** and **39** demonstrated excellent inhibitory potency against TRKA, and improved selectivity for TKRA *vs.* AURA; the profile of **39** was considered to be better than that of **38**, based on its improved KM12 potency and weaker AURA/AURB activities. Remarkably, the docking study of compound **39** exhibited an additional hydrogen bond interaction between His648 and the fluorine atom on the distal phenyl ring (Fig. 6). Interaction with His648 has been proposed to stabilize TRKA protein in the inactive state (DFG-out conformation) [31]. More importantly, **39** not only exhibited similar KM12 activity to **BPR1K871** (**10**), but also significantly decreased 50-fold IC_{50} value against AURA and AURB compared to **BPR1K871** (**10**). Hence, **39** was further pursued as a promising TRKA inhibitor.

3.4. Biological evaluation of wild-type TRKs and selectivity profile

Given the high sequence identity and similarity of the three TRK members, we further examined the enzymatic and cellular activities of lead **39** with view to better understanding its selectivity. As shown in Fig. 7, **39** demonstrated inhibitory activity against wild-type (WT) TRKA/B/C in enzymatic assays with IC_{50} values of 21.4, 29.2, 4.55 nM, respectively. Profiling of a panel of selected wild-type kinases was conducted at a screening concentration of 1 μM (Fig. 7, Table S3); the results showed that **39** is highly selective, with standard selectivity scores 0.086 (for *S* (35)) and 0.057 (*S* (10)) (Table S4). It is noteworthy that **39** also showed powerful inhibitory ability against DDR1 − the only potential off-target kinase. These data emphasize the high selectivity of lead **39** and its suitability for further *in vivo* studies and development.

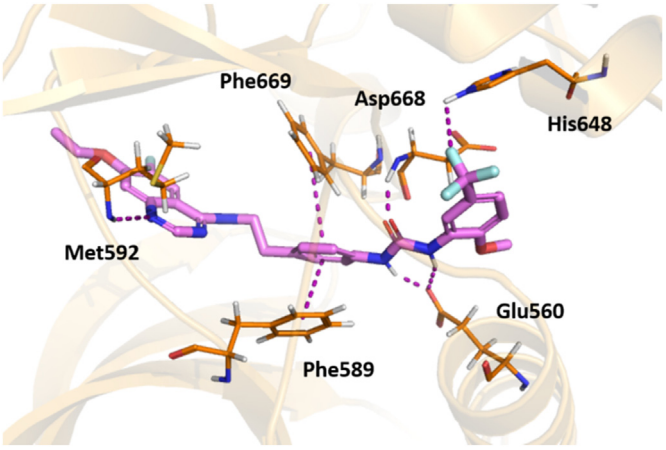

Fig. 6. Binding site analysis for lead **39** (purple) docking with TRKA X-ray protein (PDB: 6PL1, orange).

3.5. Biological evaluation of mutant forms of TRK family

There are several known NTRK gene fusions, of which $TRKA^{G595R}$ and $TRKA^{G667C}$ are the two major mutant forms of the TRKA protein; $TRKC^{G623R}$ and $TRKC^{G696A}$ are the paralogous mutant TRKC proteins. $TRKA^{F589L}$ is another amino acid substitution that has also been identified in patients who have progressed on current therapies including larotrectinib (**1**) and entrectinib (**2**) [5]. Since lead **39** exhibited promising performance in both enzymatic and cellular assays, we were interested in its ability to suppress mutant TRKA and TRKC proteins. In addition to the aforementioned NTRK gene fusions, IC_{50} values against $TRKA^{L657M}$ and $TRKC^{L686M}$ were also ascertained. Lead **39** proved to be a potent inhibitor of seven

Table 3
In Vitro TRKA kinase inhibitory activities of inhibitors **33**–**39**.[a]

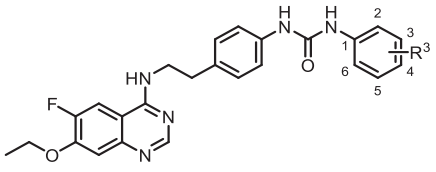

Compound	R^3	TRKA			KM12	AURA	AURB
		Inhibition @ 10 μM	Inhibition @ 1 μM	IC_{50} (nM)	IC_{50} (nM)	IC_{50} (nM)	Inhibition @ 0.5 μM
23	3-Cl	61.6%	50.7%	91.4	86.6	26.8	75%
33	H	7.9%	0.5%	> 9000	323.7	29.2	101%
34	3-F	17.4%	4.9%	4500	411.8	26.2	95%
35	3-CF_3	91.4%	88.5%	26.7	70.2	63.2	62%
36	3-Cl, 4-F	32.0%	0.6%	2630	125.2	44.0	63%
37	3-CF_3, 4-Cl	80.7%	40.9%	2120	227.9	349.4	62%
38	3-Cl, 6-OCH_3	98.0%	92.1%	23.0	95.5	351.6	511.8[a]
39	3-CF_3, 6-OCH_3	98.9%	93.7%	21.4	56.4	454.2	548.4[a]
BPR1K871 (**10**)		100%	99%	36.8	42.0	6.0	75%

[a] The IC_{50} values of AURA and inhibition values of TRKA and AURB were performed using in-house Kinase-Glo® assay; the IC_{50} values of TRKA were performed using HotSpot™ kinase assay according to the manufacturer's instructions [42]; all data are expressed as the mean of at least two independent experiments and are mostly within 15% error margins.

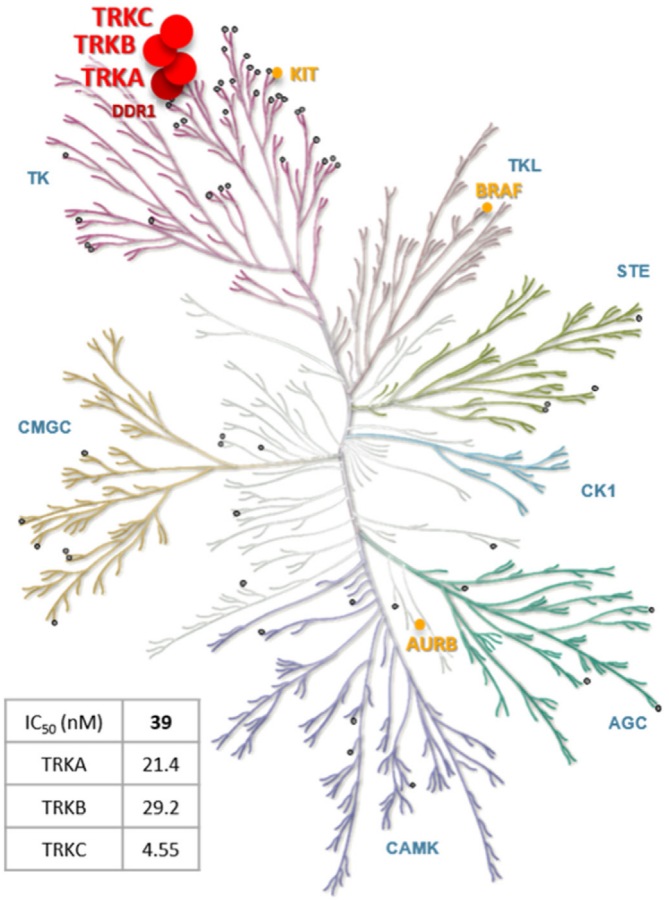

Fig. 7. Kinome-tree representation of the selectivity profile of **39** as measured by kinase inhibition assay [42]. Red dots indicate the key target TRK proteins in which the remained enzyme activity is less than 10%. A garnet dot indicates the remained enzyme activity is less than 10%. Gold dots indicate the remained enzyme activity are between 30 and 50%. Gray dots indicate the remained enzyme activity are over 50%.

mutant TRKAs and TRKCs (Table 4). Compared with larotrectinib (**1**), **39** was approximately 3–18 fold more potent an inhibitor of six mutant TRKAs and TRKCs (though not $TRKC^{G696A}$). In particular, **39** showed promising inhibitory activity against the major TRK protein mutations $TRKA^{G667C}$ and $TRKC^{G696A}$ and the gatekeeper F589L substitution of TRKA, with IC_{50} values of 13.3, 22.5, and 10.4 nM, respectively. Lead **39** even exhibited promising inhibitory activity against double-mutant TRKs such as $TRKA^{G595R/G667C}$, which has been associated with selitrectinib-treated patients [28].

On the other hand, the selectivity indices (SI; IC_{50} of $TRKA^{WT}$/mutant-TRKA) of **39** and representative compounds were evaluated and listed in Table 5. The first-generation TRKA drug, larotrectinib (**1**), is potent against wild-type TRKA protein with an IC_{50} value of 3.9 nM, but it is not capable to overcome the inevitable drug-acquired resistance with poor selectivity indices between wild-type and mutant-TRKA proteins. Two second-generation type I TRKA inhibitors, selitrectinib (**8**) and repotrectinib (**9**) exhibited extremely strong inhibitory ability against $TRKA^{WT}$, but 30-fold and 100–400-fold reduced potency against $TRKA^{G595R}$ and $TRKA^{G667C}$ enzymes, the two typical single-mutant TRKA proteins. More interestingly, both selitrectinib (**8**) and repotrectinib (**9**) are much less potent against the double-mutant $TRKA^{G595R/G667C}$ enzyme. Instead, cabozantinib (**6**) and foretinib show good ability of overcoming resistance against $TRKA^{G667C}$ and $TRKA^{G595R/G667C}$ enzymes. Being a type II TRKA inhibitor, **39** has similar performance as cabozantinib (**6**) and foretinib did. The IC_{50} values of **39** against $TRKA^{WT}$, $TRKA^{G667C}$, and $TRKA^{G595R/G667C}$ enzymes are 21.4 nM, 13.3 nM, and 19.6 nM, respectively. Differ from most of type II TRK inhibitors with multi-targeted characters, **39** is a highly selective pan-TRK inhibitor which could prevent from unexpected side effects due to off-target issues.

Table 4
Inhibitory ability of **39** against mutant TRKs.[a]

Kinase (IC_{50}, nM)	39	Larotrectinib (**1**)
$TRKA^{F589L}$	10.4	52.1
$TRKA^{G595R}$	151.4	1125
$TRKA^{G667C}$	13.3	237.2
$TRKA^{L657M}$	3.74	20.7
$TRKC^{G623R}$	75.4	208.7
$TRKC^{G696A}$	22.5	3.28
$TRKC^{L686M}$	48.4	149.7
$TRKA^{G595R/A608D}$	5.22	80.2
$TRKA^{G595R/G667C}$	19.6	> 10000
$TRKA^{G595R/L657M}$	37.6	2510

[a] The experiments were performed using HotSpot™ Kinase Assay according to the manufacturer's instructions; also, the control compound, staurosporine, was tested in 10-dose IC_{50} mode with 4-fold serial dilution starting at 20 μM [42].

3.6. Western blotting analysis

The ability of lead **39** to inhibit activation of TRKA was examined by western blotting analysis, Fig. 8. KM12 cells were treated with increasing concentrations (0–500 nM) of **39**; after 40 minutes, the autophosphorylation sites of TRKA and phospho-TRKA (Tyr490) were analyzed. The TRKA protein was found to be predominantly phosphorylated when the KM12 cells were not treated with **39**, and the amount of phospho-TRKA decreased with increasing concentrations of **39**. A concentration of about 50 nM of **39** was sufficient to suppress TRKA autophosphorylation, and **39** reduced the phosphorylation of KM12 cells in a dose-dependent manner. These data were also consistent with the antiproliferative function in KM12 cells (IC_{50} = 56.4 nM). Therefore, lead **39** was concluded to target the TRKA enzyme inside KM12 cells.

3.7. Pharmacokinetic study

The *in vivo* pharmacokinetic (PK) profile of **39** was next investigated in different species, including mice and rats (Table 6). The half-life, AUC, etc. of **39** were monitored after i.v. dosages of 1 mg/kg and 5 mg/kg, and p.o. dosages of 10 mg/kg and 20 mg/kg in mice and rats, respectively. **39** was found to exhibit acceptable drug exposure ($AUC_{(0\text{-inf})}$) and reasonable PK profiles in both species, with good oral absorption (based on AUC values) and moderate oral bioavailability of 27.9% (mice) and 27.2% (rats). These results suggest the suitability of **39** for oral administration, and spurred our evaluation of its *in vivo* efficacy.

3.8. Evaluation of in vivo efficacy of 39

The antitumor efficacy of lead **39** was evaluated in a KM12 nude mice xenograft model with a five-days-on, two-days-off (FOTO) treatment schedule. **39** was orally administered to the mice daily and the marketed TRK inhibitor larotrectinib (**1**) was utilized as a positive control. The experiment was progressed for three weeks, as shown in Fig. 9, **39** demonstrated excellent *in vivo* efficacy with the tumor growth inhibition (TGI) value of 64% at day 18. Compared with larotrectinib (**1**), lead **39** exhibited identical efficacy in the KM12 mice model. These data indicated that lead **39** is an orally efficacious TRK-inhibiting agent by delaying tumor growth.

Table 5
TRKA^{WT} and mutant-TRKA selectivity comparison between **39** and TRKA inhibitors.[a]

	39	Larotrectinib (**1**)	Selitrectinib (**8**)	Repotrectinib (**9**)	Cabozantinib (**6**)	Foretinib
TRKA^{WT} IC_{50} (nM)	21.4	3.9	0.07	0.11	72.3	2.97
TRKA^{G595R} IC_{50} (nM)	151.4	2,203	2.5	3.1	305.6	143.2
TRKA^{G667C} IC_{50} (nM)	13.3	961	30.8	10.1	1.0	0.44
TRKA$^{G595R/G667C}$ IC_{50} (nM)	19.6	> 1000	596	205	4.3	2.4
Selectivity (TRKA^{WT}/TRKA^{G595R})	0.14	0.002	0.028	0.035	0.237	0.021
Selectivity (TRKA^{WT}/TRKA^{G667C})	1.61	0.004	0.002	0.011	72.3	6.75
Selectivity (TRKA^{WT}/TRKA$^{G595R/G667C}$)	1.09	0.004	0.0001	0.0005	16.8	1.24

[a] The data of TRKA inhibitors except **39** are received from literature [31].

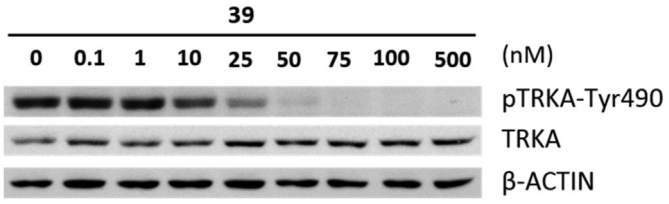

Fig. 8. Western blot analysis for cellular target modulation by **39**. Phospho-TRKA (Y490) was inhibited by **39** in KM12 cells after 40 minutes.

4. Conclusion

A series of quinazoline derivatives of varying polar surface areas and incorporating variable numbers of rotatable bonds was synthesized and evaluated in a TRKA enzymatic assay. Of these, **39** showed high enzymatic potency against TRKA, approximately 15-fold selectivity over AURA and AURB, and potent cellular activity with an IC_{50} value of 56.4 nM against the KM12 human CRC cell line expressing the chimeric TPM3-TRKA protein. Molecular docking studies revealed that **39** conducted a type II binding mode, which especially interacted with the His648 in the back pockets of TRKA kinase – a crucial interaction stabilizes the DFG-out conformation. More importantly, **39** exhibited significantly improved drug-like properties (NRB and PSA) compared to our previously reported candidate **BPR1K871** (**10**), as well as good AUC and oral bioavailability (F = 27.9% for mice and 27.2% for rats), and excellent *in vivo* efficacy (TGI of 64% at day 18) in a KM12 mice xenograft model. Finally, **39** demonstrated broad-spectrum potency (IC_{50} = 3.74–151.4 nM) against mutant TRKAs and TRKCs, and, in particular, was 3–65 fold more potent an inhibitor than larotrectinib (**1**), especially of double-mutant TRKAs. Accordingly, **39** is considered a next-generation orally selective type II TRK inhibitor as a potential candidate for the treatment of rare cancers incorporating NTRK gene fusions.

5. Experimental section

5.1. General methods for chemistry

All commercial chemicals and solvents are of reagent grade and were used without further purification unless otherwise stated. All reactions were carried out under dry nitrogen or argon atmosphere and were monitored for completion by TLC using Merck 60 F_{254} silica gel glass-backed plates; zones were detected visually under UV irradiation (254 nm) or by spraying with potassium permanganate reagent (Aldrich) followed by heating at 80 °C. Flash column chromatography was carried out using silica gel (Silicycle SiliaFlash® P60, R12030B, 230–400 mesh). ^{1}H and ^{13}C NMR spectra were recorded with Varian Mercury-300 or Varian Mercury-400 spectrometers or Bruker 400 MHz or 600 MHz AVANCE III spectrometers and the chemical shifts were recorded in parts per million (ppm, δ) and reported relative to the solvent peak. Data analysis was done using Mnova software. Low-resolution mass spectra (LRMS) data were measured with Agilent MSD-1100 ESI-MS/MS system. High-resolution mass spectra (HRMS) data were

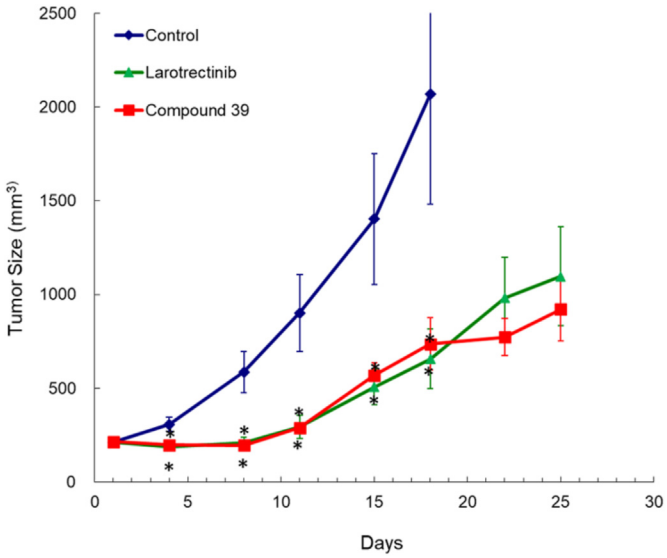

Fig. 9. *In vivo* antitumor efficacy of compound **39** and larotrectinib (**1**) in the KM12 xenograft mouse model. Compound **39** was orally administered to the mice at a dosage of 100 mg/kg once a day for three days (days 1–3), whereupon the dosage was reduced to 75 mg/kg due to observed body weight loss (days 4–5); then the optimum dosage and dosing schedule were finally determined to be three times per week at 75 mg/kg. Larotrectinib (**1**) at a dosage of 75 mg/kg dosage was utilized as a positive control.

Table 6
Pharmacokinetic profile of compound **39** in mice and rats.

Species	i.v.				p.o.				
	$t_{1/2}$ (h)	CL (ml/min/kg)	V_{ss} (l/kg)	$AUC_{(0\text{-inf})}$ (ng/mL × hr)	$t_{1/2}$ (h)	C_{max} (ng/ml)	T_{max} (h)	$AUC_{(0\text{-inf})}$ (ng/mL × hr)	F (%)
mice[a]	2.9	7.4	0.6	5081	2.2	2406	1.7	5793	27.9
rat[b]	5.3	12.2	2.3	2772	5.1	454.7	4.3	3012	27.2

[a] The dosage of i.v. is 1 mg/kg and the dosage of p.o. is 10 mg/kg.
[b] The dosage of i.v. is 5 mg/kg and the dosage of p.o. is 20 mg/kg.

measured with Varian 901-MS FT-ICR HPLC/MS-MS system. Purity of the final compounds were determined with a Hitachi 2000 series HPLC system using C-18 column (Agilent ZORBAX Eclipse XDB-C18 5 μm. 4.6 mm × 150 mm) operating at 25 °C. The elution was carried out using acetonitrile as mobile phase A, and water containing 0.1% formic acid + 2 mmol NH_4OAc as mobile phase B. Elution conditions: at 0 min, phase A 10% + phase B 90%; at 25 min, phase A 90% + phase B 10%; at 30 min, phase A 90% + phase B 10%; at 30.5 min, phase A 10% + phase B 90%; at 37 min, phase A 10% + phase B 90%. The flow-rate of the mobile phase was 0.5 mL/min and the injection volume of the sample was 10 or 20 μL. Peaks were detected at 254 nm. IUPAC nomenclature of compounds were obtained with the software ACD/Name Pro.

General Procedure A. To a solution of the 4-chloropyrimidine derivatives **11a**–**f** (1.0 equiv.) in appropriate alcohol type solution (1.0–20.0 mL) was added appropriate aniline (1.1–3.0 equiv.) and triethylamine (0–1.9 equiv.) then the reaction mixture was stirred at reflux. After stirred for 1–12 h, the reaction mixture was cooled down to room temperature, concentrated *in vacuo* and purified by silica gel column chromatography using the appropriate mobile phase to yield the title compounds **19a**–**f**.

General Procedure B. To a solution of amine derivatives **19a**–**f** (1.0 equiv.) in dichloromethane (0.5–30 mL) or *N,N*-dimethylformamide (1 mL) and was added appropriate isocyanate (1.0–2.1 equiv.) and methanol (0–0.20 mL) then the reaction mixture was stirred at room temperature. After stirred for 1–16 h, the resulting precipitate was collected, washed with dichloromethane (5–20 mL) and dried *in vacuo* to yield the title compounds **20**–**23**, **25**–**39** in 28–98% yield.

1-(5-{2-[(6,7-Dimethoxyquinazolin-4-yl*)amino]ethyl}-1,3-thiazol*-2-yl*)-3-phenylurea (**16**).* To a solution of **13c** (208 mg, 0.63 mmol, 1.0 equiv.) in dichloromethane (3.0 mL) was added phenyl isocyanate (97 mg, 0.82 mmol, 1.3 equiv.) and methanol (0.3 mL) then the reaction mixture was stirred at room temperature. After stirred for 4 h, the reaction mixture was concentrated *in vacuo* and purified by column chromatography (2–5% methanol/dichloromethane) to yield the title compound **16** (165 mg, 0.37 mmol, 58%) as white solid. ^{1}H NMR (400 MHz, DMSO-d_6) δ 10.34 (br s, 1H), 8.97 (s, 1H), 8.37 (s, 1H), 8.11 (t, J = 5.6 Hz, 1H), 7.59 (s, 1H), 7.45 (d, J = 8.0 Hz, 1H), 7.31 (dd, J = 8.0, 7.4 Hz, 2H), 7.13 (s, 1H), 7.10 (s, 1H), 7.02 (t, J = 7.4 Hz, 1H), 3.90 (s, 3H), 3.89 (s, 3H), 3.41 (td, J = 7.0, 5.6 Hz, 2H), 3.08 (t, J = 7.0 Hz, 2H). ^{13}C NMR (150 MHz, DMSO-d_6) δ 158.4, 154.2, 152.9, 151.9, 148.7, 144.3, 138.9, 134.0, 129.0, 127.7, 122.7, 118.6, 108.4, 106.0, 102.2, 56.1, 55.8, 42.0, 26.0. LC-MS (ESI) m/z: 451.2 $[M+H]^+$. HRMS (ESI) m/z: calcd for $C_{22}H_{23}N_6O_3S$, 451.1552 $[M+H]^+$, found 451.1560. HPLC purity: 99.5%, t_R = 13.97 min.

*N-[2-(4-Aminophenyl)ethyl]-7-(3-chloropropoxy)quinazolin-4-amine (**19a**).* The title compound was synthesized following the general procedure A and using the reactants/reagents **11a** (200 mg, 0.78 mmol, 1.0 equiv.), 4-(2-aminoethyl)aniline (127 mg, 0.93 mmol, 1.2 equiv.), triethylamine (118 mg, 1.17 mmol, 1.5 equiv.) and ethanol (5.0 mL). After stirred at reflux for 1 h and work-up, the title compound **19a** was obtained in 40% yield as light yellow solid. ^{1}H NMR (300 MHz, CD_3OD-d_4) δ 8.37 (s, 1H), 7.95 (dd, J = 9.0, 0.6 Hz, 1H), 7.11 (dd, J = 9.0, 2.6 Hz, 1H), 7.07 (d, J = 2.6 Hz, 1H), 7.01 (d, J = 8.6 Hz, 2H), 6.68 (d, J = 8.6 Hz, 2H), 4.25 (t, J = 6.0 Hz, 2H), 3.84–3.69 (m, 4H), 2.87 (t, J = 7.5 Hz, 2H), 2.29 (tt, J = 6.0, 6.0 Hz, 2H). LC-MS (ESI) m/z: 357.1 $[M+H]^+$.

*N-[2-(4-Aminophenyl)ethyl]-7-ethoxy-6-fluoroquinazolin-4-amine (**19d**).* The title compound was synthesized following the general procedure A and using the reactants/reagents **11d** (453 mg, 2.00 mmol, 1.0 equiv.), 4-(2-aminoethyl)aniline (331 mg, 2.43 mmol, 1.2 equiv.) and ethanol (10.0 mL). After stirred at reflux for 1 h and work-up, the title compound **19d** was obtained in 60% yield as pale orange solid. ^{1}H NMR (300 MHz, DMSO-d_6) δ 8.41 (s, 1H), 8.13–8.00 (m, 2H), 7.24 (d, J = 8.4 Hz, 1H), 6.90 (d, J = 8.3 Hz, 2H), 6.49 (d, J = 8.3 Hz, 2H), 4.86 (s, 2H), 4.24 (q, J = 7.1 Hz, 2H), 3.62 (td, J = 8.1, 6.3 Hz, 2H), 2.74 (t, J = 8.1 Hz, 2H), 1.41 (t, J = 7.1 Hz, 3H). LC-MS (ESI) m/z: 327.2 $[M+H]^+$.

*N-(4-Aminobenzyl)-7-ethoxy-6-fluoroquinazolin-4-amine (**19d'**).* The title compound was synthesized following the general procedure A and using the reactants/reagents **11d** (150 mg, 0.66 mmol, 1.0 equiv.), 4-(aminomethyl)aniline (86 mg, 0.80 mmol, 1.2 equiv.) and ethanol (3.0 mL). After stirred at reflux for 12 h and work-up, the title compound **19d'** was obtained in 73% yield as khaki solid. ^{1}H NMR (400 MHz, DMSO-d_6) δ 8.43–8.32 (m, 2H), 8.15 (d, J = 12.4 Hz, 1H), 7.25 (d, J = 8.4 Hz, 1H), 7.02 (d, J = 8.2 Hz, 2H), 6.50 (d, J = 8.2 Hz, 2H), 4.97 (br s, 2H), 4.56 (d, J = 5.6 Hz, 2H), 4.24 (q, J = 7.0 Hz, 2H), 1.40 (t, J = 7.0 Hz, 3H). LC-MS (ESI) m/z: 313.3 $[M+H]^+$.

N-(7-Ethoxy-6-fluoroquinazolin-4-yl*)benzene-1,4-diamine (**19d"**).* The title compound was synthesized following the general procedure A and using the reactants/reagents **11d** (150 mg, 0.66 mmol, 1.0 equiv.), benzene-1,4-diamine (79 mg, 0.73 mmol, 1.1 equiv.) and propan-2-ol (1.0 mL). After stirred at reflux for 1 h and work-up, the title compound **19d"** was obtained in 97% yield as khaki solid. ^{1}H NMR (400 MHz, DMSO-d_6) δ 8.68 (s, 1H), 8.52 (d, J = 11.6 Hz, 1H), 7.43 (d, J = 8.0 Hz, 2H), 7.35 (d, J = 8.0 Hz, 1H), 6.78 (d, J = 8.4 Hz, 2H), 4.31 (q, J = 7.0 Hz, 2H), 1.45 (t, J = 7.0 Hz, 3H). LC-MS (ESI) m/z: 299.1 $[M+H]^+$.

*N-[2-(4-Aminophenyl)ethyl]-6,7-difluoroquinazolin-4-amine (**19d"**).* The title compound was synthesized following the general procedure A and using the reactants/reagents **11e** (310 mg, 1.55 mmol, 1.0 equiv.), 4-(2-aminoethyl)aniline (634 mg, 4.66 mmol, 3.0 equiv.), triethylamine (305 mg, 3.01 mmol, 1.9 equiv.) and propan-2-ol (1.3 mL). After stirred at reflux for 1 h and work-up, the title compound **19e** was obtained in 85% yield as white solid. ^{1}H NMR (400 MHz, DMSO-d_6) δ 8.48 (s, 1H), 8.38–8.29 (m, 2H), 7.69 (dd, J = 12.0, 8.0 Hz, 1H), 6.90 (d, J = 8.2 Hz, 2H), 6.49 (d, J = 8.2 Hz, 2H), 4.87 (s, 2H), 3.64 (td, J = 8.2, 6.0 Hz, 2H), 2.76 (t, J = 8.2 Hz, 2H). LC-MS (ESI) m/z: 301.1 $[M+H]^+$.

*N-[2-(4-Aminophenyl)ethyl]-6-ethoxy-7-fluoroquinazolin-4-amine (**19f**).* The title compound was synthesized following the general procedure A and using the reactants/reagents **11f** (165 mg, 0.73 mmol, 1.0 equiv.), 4-(2-aminoethyl)aniline (119 mg, 0.87 mmol, 1.2 equiv.) and ethanol (3.6 mL). After stirred at reflux for 1 h and work-up, the title compound **19f** was obtained in 72% yield as pale yellow solid. ^{1}H NMR (400 MHz, DMSO-d_6) δ 8.39 (s, 1H), 8.22 (t, J = 5.2 Hz, 1H), 7.82 (d, J = 9.2 Hz, 1H), 7.45 (d, J = 12.4 Hz, 1H), 6.91 (d, J = 8.0 Hz, 2H), 6.50 (d, J = 8.0 Hz, 2H), 4.87 (s, 2H), 4.21 (q, J = 6.8 Hz, 2H), 3.64 (td, J = 8.2, 6.0 Hz, 2H), 2.77 (t, J = 8.2 Hz, 2H), 1.43 (t, J = 6.8 Hz, 3H). LC-MS (ESI) m/z: 327.2 $[M+H]^+$.

1-[4-(2-{[7-(3-Chloropropoxy)quinazolin-4-yl*]amino}ethyl)phenyl]-3-phenylurea (**20**).* The title compound was synthesized following the general procedure B and using the reactants/reagents **19a** (2.00 g, 5.60 mmol, 1.0 equiv.), phenyl isocyanate (1.33 g, 11.2 mmol, 2.0 equiv.) and dichloromethane (30 mL). After stirred at room temperature overnight and work-up, the title compound **20** was obtained in 71% yield as light yellow solid. ^{1}H NMR (300 MHz, DMSO-d_6) δ 8.66 (s, 1H), 8.62 (s, 1H), 8.42 (s, 1H), 8.20 (t, J = 6.0 Hz, 1H), 8.13 (d, J = 8.4 Hz, 1H), 7.44 (d, J = 8.6, 1.1 Hz, 2H), 7.37 (d, J = 8.6 Hz, 2H), 7.27 (dd, J = 8.6, 7.5 Hz, 2H), 7.16 (d, J = 8.6 Hz, 2H), 7.14 (d, J = 2.7 Hz, 1H), 7.10 (dd, J = 8.4, 2.7 Hz, 1H), 6.95 (tt, J = 7.5, 1.1 Hz, 1H), 4.23 (t, J = 6.2 Hz, 2H), 3.82 (t, J = 6.5 Hz, 2H), 3.70 (td, J = 7.8, 6.0 Hz, 2H), 2.89 (t, J = 7.8 Hz, 2H), 2.22 (tt, J = 6.5, 6.2 Hz, 2H). LC-MS (ESI) m/z: 476.2 $[M+H]^+$.

*1-Phenyl-3-{4-[2-(quinazolin-4-ylamino)ethyl]phenyl}urea (**21**).* The title compound was synthesized following the general

procedure B and using the reactants/reagents **19b** (200 mg, 0.76 mmol, 1.0 equiv.), isocyanatobenzene (135 mg, 1.13 mmol, 1.5 equiv.) and dichloromethane (20 mL). After stirred for 8 h at room temperature and work-up, the title compound **21** was obtained in 98% yield as pale yellow solid. ^{1}H NMR (400 MHz, DMSO-d_6) δ 8.61 (s, 1H), 8.58 (s, 1H), 8.49 (s, 1H), 8.38 (t, J = 6.0 Hz, 1H), 8.21 (d, J = 8.0 Hz, 1H), 7.78 (ddd, J = 8.0, 6.8, 1.2 Hz, 1H), 7.67 (dd, J = 8.4, 1.2 Hz, 1H), 7.50 (ddd, J = 8.4, 6.8, 1.2 Hz, 1H), 7.44 (d, J = 7.8 Hz, 2H), 7.37 (d, J = 8.4 Hz, 2H), 7.27 (dd, J = 7.8, 7.6 Hz, 2H), 7.18 (d, J = 8.4 Hz, 2H), 6.95 (t, J = 7.6 Hz, 1H), 3.73 (td, J = 7.6, 6.0 Hz, 2H), 2.91 (t, J = 7.6 Hz, 2H). ^{13}C NMR (150 MHz, DMSO-d_6) δ 159.3, 155.2, 152.6, 149.1, 139.8, 137.8, 132.9, 132.4, 129.0, 128.8, 127.5, 125.5, 122.6, 121.7, 118.4, 118.2, 115.0, 42.3, 33.9. LC-MS (ESI) m/z: 384.3 [M+H]$^+$. HRMS (ESI) m/z: calcd for $C_{23}H_{14}N_1O_5$, 384.0872 [M+H]$^+$, found 384.0871. HPLC purity: 97.9%, t_R = 20.82 min.

1-(3-Chlorophenyl)-3-(4-{2-[(7-ethoxy-6-fluoroquinazolin-4-yl*)amino]ethyl}phenyl)urea (**23**).* The title compound was synthesized following the general procedure B and using the reactants/reagents **19d** (130 mg, 0.40 mmol, 1.0 equiv.), 1-chloro-3-isocyanatobenzene (88 mg, 0.58 mmol, 1.4 equiv.), methanol (0.13 mL) and dichloromethane (13 mL). After work-up, the title compound **23** was obtained in 46% yield as white solid. ^{1}H NMR (400 MHz, DMSO-d_6) δ 8.87 (s, 1H), 8.70 (s, 1H), 8.43 (s, 1H), 8.14–8.02 (m, 2H), 7.71 (dd, J = 2.4, 1.6 Hz, 1H) 7.38 (d, J = 8.6 Hz, 2H), 7.34–7.24 (m, 3H), 7.18 (d, J = 8.6 Hz, 1H), 7.00 (ddd, J = 8.0, 1.6, 1.6 Hz, 1H), 4.24 (q, J = 7.0 Hz, 2H), 3.70 (td, J = 7.8, 6.0 Hz, 2H), 2.89 (t, J = 7.8 Hz, 2H), 1.41 (t, J = 7.0 Hz, 3H). ^{13}C NMR (150 MHz, DMSO-d_6) δ 158.7 (d, $J_{C\text{-}F}$ = 3.5 Hz), 155.1, 152.4, 151.0 (d, $J_{C\text{-}F}$ = 12.8 Hz), 150.1 (d, $J_{C\text{-}F}$ = 245.1 Hz), 147.8, 141.3, 137.5, 133.18, 133.16, 130.3, 129.0, 121.3, 118.5, 117.5, 116.5, 109.7, 108.0 (d, $J_{C\text{-}F}$ = 7.4 Hz), 107.7 (d, $J_{C\text{-}F}$ = 20.0 Hz), 64.5, 42.2, 33.9, 14.3. LC-MS (ESI) m/z: 480.2 [M+H]$^+$. HRMS (ESI) m/z: calcd for $C_{25}H_{24}ClFN_5O_2$, 480.1603 [M+H]$^+$, found 480.1600. HPLC purity: 99.3%, t_R = 18.95 min.

1-{4-[2-({7-[3-(Dimethylamino)propoxy]quinazolin-4-yl*}amino)ethyl]phenyl}-3-phenylurea (**24**).* To a solution of **20** (1.46 g, 3.07 mmol, 1.0 equiv.) in *N*,*N*-dimethylacetamide (10 mL) was added a solution of dimethylamine in water (6.91 mg, 61.34 mmol, 20.0 equiv.) then the reaction was heated at 120 °C under microwave irradiation. After stirred for 100 min, the reaction mixture was cooled down and poured into an ice bath. The resulting precipitate was collected, washed with water (50 mL) and acetone (20 mL). Then the crude product was purified by silica gel column chromatography to yield the title compound **24** in 64% yield as white solid. ^{1}H NMR (400 MHz, DMSO-d_6) δ 8.69 (s, 1H), 8.65 (s, 1H), 8.41 (s, 1H), 8.19 (t, J = 5.8 Hz, 1H), 8.11 (d, J = 9.0 Hz, 1H), 7.44 (dd, J = 8.6, 1.2 Hz, 2H), 7.37 (d, J = 8.4 Hz, 2H), 7.27 (dd, J = 8.6, 7.2 Hz, 2H), 7.17 (d, J = 8.4 Hz, 2H), 7.10 (dd, J = 9.0, 2.8 Hz, 1H), 7.04 (d, J = 2.8 Hz, 1H), 6.95 (tt, J = 7.2, 1.2 Hz, 1H), 4.12 (t, J = 6.6 Hz, 2H), 3.70 (td, J = 8.0, 5.8 Hz, 2H), 2.88 (t, J = 8.0 Hz, 2H), 2.38 (t, J = 7.0 Hz, 2H), 2.16 (s, 6H), 1.89 (tt, J = 7.0, 6.6 Hz, 2H). ^{13}C NMR (150 MHz, DMSO-d_6) δ 161.6, 159.0, 155.7, 152.6, 151.4, 139.8, 137.8, 132.9, 129.0, 128.7, 124.2, 121.7, 118.3, 118.1, 116.8, 109.1, 107.5, 66.0, 55.5, 45.0, 42.2, 34.0, 26.6. LC-MS (ESI) m/z: 485.3 [M+H]$^+$. HRMS (ESI) m/z: calcd for $C_{28}H_{33}N_6O_2$, 485.2665 [M+H]$^+$, found 485.2663. HPLC purity: 98.2%, t_R = 17.35 min.

1-(4-{[(7-Ethoxy-6-fluoroquinazolin-4-yl*)amino]methyl}phenyl)-3-phenylurea (**25**).* The title compound was synthesized following the general procedure B and using the reactants/reagents **19d'** (70 mg, 0.22 mmol, 1.0 equiv.), isocyanatobenzene (55 mg, 0.46 mmol, 2.1 equiv.) and dichloromethane (1 mL). After stirred for 16 h at room temperature and work-up, the title compound **25** was obtained in 43% yield as creamy-white solid. ^{1}H NMR (400 MHz, DMSO-d_6) δ 8.65 (s, 1H), 8.61 (s, 1H), 8.51 (t, J = 5.6 Hz, 1H), 8.40 (s, 1H), 8.16 (d, J = 12.4 Hz, 1H), 7.46–7.36 (m, 4H), 7.31–7.22 (m, 5H), 6.95 (t, J = 7.2 Hz, 1H), 4.69 (d, J = 5.6 Hz, 2H), 4.25 (q, J = 6.8 Hz, 2H), 1.41 (t, J = 6.8 Hz, 3H). ^{13}C NMR (100 MHz, DMSO-d_6) δ 158.7 (d, $J_{C\text{-}F}$ = 4.3 Hz), 155.1, 152.5, 151.1 (d, $J_{C\text{-}F}$ = 12.9 Hz), 150.2 (d, $J_{C\text{-}F}$ = 245.5 Hz), 148.0, 139.7, 138.5, 132.7, 128.7, 127.9, 121.7, 118.2, 118.1, 109.7, 107.9 (d, $J_{C\text{-}F}$ = 6.3 Hz), 107.8, 64.6, 43.2, 14.3. LC-MS (ESI) m/z: 432.4 [M+H]$^+$. HRMS (ESI) m/z: calcd for $C_{24}H_{23}FN_5O_2$, 432.1836 [M+H]$^+$, found 432.1835. HPLC purity: 90.9%, t_R = 16.57 min.

1-(3-Chlorophenyl)-3-(4-{[(7-ethoxy-6-fluoroquinazolin-4-yl*)amino]methyl}phenyl)urea (**26**).* The title compound was synthesized following the general procedure B and using the reactants/reagents **19d'** (50 mg, 0.16 mmol, 1.0 equiv.), 1-chloro-3-isocyanatobenzene (25 mg, 0.16 mmol, 1.0 equiv.) and dichloromethane (1 mL). After stirred for 16 h at room temperature and work-up, the title compound **26** was obtained in 90% yield as pale yellow solid. ^{1}H NMR (400 MHz, DMSO-d_6) δ 8.87 (s, 1H), 8.75 (s, 1H), 8.52 (t, J = 5.8 Hz, 1H), 8.41 (s, 1H), 8.15 (d, J = 12.4 Hz, 1H), 7.71 (dd, J = 2.0, 1.6 Hz, 1H), 7.41 (d, J = 8.8 Hz, 2H), 7.33–7.20 (m, 5H), 6.82 (ddd, J = 6.8, 2.0, 2.0 Hz, 1H), 4.70 (d, J = 5.8 Hz, 2H), 4.22 (q, J = 7.0 Hz, 2H), 1.40 (t, J = 7.0 Hz, 3H). ^{13}C NMR (150 MHz, DMSO-d_6) δ 158.7 (d, $J_{C\text{-}F}$ = 2.1 Hz), 155.0, 152.4, 151.2 (d, $J_{C\text{-}F}$ = 12.8 Hz), 150.2 (d, $J_{C\text{-}F}$ = 245.4 Hz), 148.0, 141.3, 138.2, 133.2, 133.0, 130.3, 127.9, 121.4, 118.4, 117.5, 116.6, 109.7, 108.0 (d, $J_{C\text{-}F}$ = 8.4 Hz), 107.9 (d, $J_{C\text{-}F}$ = 20.6 Hz), 64.6, 43.2, 14.3. LC-MS (ESI) m/z: 466.4 [M+H]$^+$. HRMS (ESI) m/z: calcd for $C_{24}H_{22}ClFN_5O_2$, 466.1446 [M+H]$^+$, found 466.1446. HPLC purity: 95.2%, t_R = 18.60 min.

1-{4-[(7-Ethoxy-6-fluoroquinazolin-4-yl*)amino]phenyl}-3-phenylurea (**27**).* The title compound was synthesized following the general procedure B and using the reactants/reagents **19d"** (33 mg, 0.11 mmol, 1.0 equiv.), isocyanatobenzene (27 mg, 0.23 mmol, 2.1 equiv.) and dichloromethane (0.5 mL). After stirred for 16 h at room temperature and work-up, the title compound **27** was obtained in 28% yield as pale yellow solid. ^{1}H NMR (400 MHz, DMSO-d_6) δ 9.51 (s, 1H), 8.66 (s, 1H), 8.65 (s, 1H), 8.49 (s, 1H), 8.40 (d, J = 12.8 Hz, 1H), 7.69 (d, J = 8.8 Hz, 2H), 7.50–7.42 (m, 4H), 7.34 (d, J = 8.4 Hz, 1H), 7.28 (dd, J = 8.0, 7.6 Hz, 2H), 6.97 (t, J = 7.6 Hz, 1H), 4.28 (q, J = 7.0 Hz, 2H), 1.43 (t, J = 7.0 Hz, 3H). ^{13}C NMR (150 MHz, DMSO-d_6) δ 157.1, 154.6, 152.6, 151.4 (d, $J_{C\text{-}F}$ = 13.1 Hz), 150.5 (d, $J_{C\text{-}F}$ = 245.6 Hz), 148.5, 139.8, 135.7, 133.2, 128.8, 123.0, 121.7, 118.3, 118.1, 109.9, 108.2 (d, $J_{C\text{-}F}$ = 7.7 Hz), 108.0 (d, $J_{C\text{-}F}$ = 20.3 Hz), 64.7, 14.3. LC-MS (ESI) m/z: 418.4 [M+H]$^+$. HRMS (ESI) m/z: calcd for $C_{23}H_{21}FN_5O_2$, 418.1679 [M+H]$^+$, found 418.1786. HPLC purity: 98.9%, t_R = 16.57 min.

1-(3-Chlorophenyl)-3-{4-[(7-ethoxy-6-fluoroquinazolin-4-yl*)amino]phenyl}urea (**28**).* The title compound was synthesized following the general procedure B and using the reactants/reagents **19d"** (100 mg, 0.34 mmol, 1.0 equiv.), 1-chloro-3-isocyanatobenzene (63 mg, 0.41 mmol, 1.2 equiv.) and dichloromethane (1 mL). After stirred for 2 h at room temperature and work-up, the title compound **28** was obtained in 46% yield as pale yellow solid. ^{1}H NMR (400 MHz, DMSO-d_6) δ 9.56 (s, 1H), 8.94 (s, 1H), 8.80 (s, 1H), 8.51 (s, 1H), 8.42 (d, J = 12.8 Hz, 2H), 7.75–7.67 (m, 3H), 7.47 (d, J = 8.8 Hz, 2H), 7.38–7.24 (m, 3H), 7.01 (ddd, J = 7.2, 2.0, 2.0 Hz, 1H), 4.29 (q, J = 6.8 Hz, 2H), 1.43 (t, J = 6.8 Hz, 3H). ^{13}C NMR (150 MHz, DMSO-d_6) δ 157.1, 154.4, 152.5, 151.4 (d, $J_{C\text{-}F}$ = 13.1 Hz), 150.5 (d, $J_{C\text{-}F}$ = 245.9 Hz), 148.3, 141.4, 135.4, 133.4, 133.2, 123.0, 121.3, 118.5, 117.4, 116.5, 109.7, 108.2, 108.1 (d, $J_{C\text{-}F}$ = 20.6 Hz), 64.7, 14.3. LC-MS (ESI) m/z: 452.3 [M+H]$^+$. HRMS (ESI) m/z: calcd for $C_{23}H_{20}ClFN_5O_2$, 452.1290 [M+H]$^+$, found 452.1323. HPLC purity: 97.1%, t_R = 19.59 min.

1-(3-Chlorophenyl)-3-(4-{2-[(6,7-difluoroquinazolin-4-yl*)amino]ethyl}phenyl)urea (**29**).* The title compound was synthesized following the general procedure B and using the reactants/reagents **19e** (60 mg, 0.20 mmol, 1.0 equiv.), isocyanatobenzene (29 mg, 0.24 mmol, 1.2 equiv.) and dichloromethane (5.0 mL). After stirred for 90 min at room temperature and work-up, the title compound

29 was obtained in 88% yield as white solid. ^{1}H NMR (400 MHz, DMSO-d_6) δ 8.70 (s, 1H), 8.67 (s, 1H), 8.50 (s, 1H), 8.41–8.29 (m, 2H), 7.70 (dd, J = 11.6, 8.0 Hz, 1H) 7.44 (d, J = 7.6 Hz, 2H), 7.38 (d, J = 8.4 Hz, 2H), 7.26 (dd, J = 7.8, 7.6 Hz, 2H), 7.17 (d, J = 8.4 Hz, 2H), 6.95 (t, J = 7.8 Hz, 1H), 3.72 (td, J = 7.8, 6.4 Hz, 2H), 2.89 (t, J = 7.8 Hz, 2H). ^{13}C NMR (150 MHz, DMSO-d_6) δ 158.8, 155.8, 152.9 (dd, $J_{C\text{-}F}$ = 252.0, 15.2 Hz), 152.5, 147.8 (dd, $J_{C\text{-}F}$ = 246.0, 14.2 Hz), 147.3 (d, $J_{C\text{-}F}$ = 11.3 Hz), 139.8, 137.9, 132.6, 129.0, 128.7, 121.7, 118.3, 118.1, 114.4 (d, $J_{C\text{-}F}$ = 16.1 Hz), 111.6 (d, $J_{C\text{-}F}$ = 6.6 Hz), 110.1 (d, $J_{C\text{-}F}$ = 18.6 Hz), 42.3, 33.7. LC-MS (ESI) m/z: 420.2 $[M+H]^+$. HRMS (ESI) m/z: calcd for $C_{23}H_{20}F_2N_5O$, 420.1636 $[M+H]^+$, found 420.1622. HPLC purity: 95.9%, t_R = 17.77 min.

1-(4-{2-[(6,7-Difluoroquinazolin-4-yl*)amino]ethyl}phenyl)-3-phenylurea (**30**).* The title compound was synthesized following the general procedure B and using the reactants/reagents **19e** (60 mg, 0.20 mmol, 1.0 equiv.), 1-chloro-3-isocyanatobenzene (37 mg, 0.24 mmol, 1.2 equiv.) and dichloromethane (6 mL). After stirred for 90 min at room temperature and work-up, the title compound **30** was obtained in 99% yield as white solid. ^{1}H NMR (400 MHz, DMSO-d_6) δ 8.89 (s, 1H), 8.72 (s, 1H), 8.50 (s, 1H), 8.41–8.29 (m, 2H), 7.74–7.66 (m, 2H), 7.38 (d, J = 8.4 Hz, 2H) 7.32–7.22 (m, 2H), 7.18 (d, J = 8.4 Hz, 2H), 7.00 (ddd, J = 7.6, 2.0, 2.0 Hz, 1H), 3.72 (td, J = 7.6, 6.0 Hz, 2H), 2.90 (t, J = 7.6 Hz, 2H). ^{13}C NMR (150 MHz, DMSO-d_6) δ 158.8, 155.8, 152.9 (dd, $J_{C\text{-}F}$ = 251.8, 15.2 Hz), 152.4, 147.8 (dd, $J_{C\text{-}F}$ = 254.2, 14.5 Hz), 147.3 (d, $J_{C\text{-}F}$ = 11.0 Hz), 141.3, 137.6, 133.2, 133.0, 130.3, 129.0, 121.3, 118.5, 117.4, 116.5, 114.4 (d, $J_{C\text{-}F}$ = 15.9 Hz), 111.6 (d, $J_{C\text{-}F}$ = 6.0 Hz), 110.1 (d, $J_{C\text{-}F}$ = 18.8 Hz), 42.3, 33.7. LC-MS (ESI) m/z: 454.2 $[M+H]^+$. HRMS (ESI) m/z: calcd for $C_{23}H_{19}ClF_2N_5O$, 454.1246 $[M+H]^+$, found 454.1254. HPLC purity: 94.2%, t_R = 20.77 min.

1-(4-{2-[(6-Ethoxy-7-fluoroquinazolin-4-yl*)amino]ethyl}phenyl)-3-phenylurea (**31**).* The title compound was synthesized following the general procedure B and using the reactants/reagents **19f** (114 mg, 0.35 mmol, 1.0 equiv.), phenyl isocyanate (55 mg, 0.46 mmol, 1.3 equiv.), methanol (0.1 mL) and dichloromethane (10 mL). After stirred at room temperature for 1 h and work-up, the title compound **31** was obtained in 87% yield as white solid. ^{1}H NMR (400 MHz, DMSO-d_6) δ 8.61 (s, 1H), 8.58 (s, 1H), 8.41 (s, 1H), 8.26 (t, J = 5.6 Hz, 1H), 7.83 (d, J = 8.8 Hz, 1H), 7.50–7.41 (m, 3H), 7.38 (d, J = 8.2 Hz, 2H), 7.27 (dd, J = 8.2, 7.4 Hz, 2H), 7.18 (d, J = 8.2 Hz, 2H), 6.96 (t, J = 7.4 Hz, 1H), 4.17 (q, J = 7.0 Hz, 2H), 3.72 (td, J = 7.8, 5.6 Hz, 2H), 2.90 (t, J = 7.8 Hz, 2H), 1.43 (t, J = 7.0 Hz, 3H). ^{13}C NMR (100 MHz, DMSO-d_6) δ 158.4, 155.3 (d, $J_{C\text{-}F}$ = 251.7 Hz), 154.2, 152.6, 145.7 (d, $J_{C\text{-}F}$ = 12.4 Hz), 144.9 (d, $J_{C\text{-}F}$ = 11.8 Hz), 139.8, 137.9, 132.9, 129.0, 128.8, 121.8, 118.4, 118.2, 112.6 (d, $J_{C\text{-}F}$ = 17.3 Hz), 111.9, 105.3 (d, $J_{C\text{-}F}$ = 2.4 Hz), 64.9, 42.4, 34.1, 14.4. LC-MS (ESI) m/z: 446.3 $[M+H]^+$. HRMS (ESI) m/z: calcd for $C_{25}H_{25}FN_5O_2$, 446.1992 $[M+H]^+$, found 446.1986. HPLC purity: 95.5%, t_R = 17.35 min.

1-(3-Chlorophenyl)-3-(4-{2-[(6-ethoxy-7-fluoroquinazolin-4-yl*)amino]ethyl}phenyl)urea (**32**).* The title compound was synthesized following the general procedure B and using the reactants/reagents **19f** (94 mg, 0.29 mmol, 1.0 equiv.), 1-chloro-3-isocyanatobenzene (53 mg, 0.35 mmol, 1.2 equiv.) and *N*,*N*-dimethylacetamide (1 mL). After stirred at room temperature for 2 h and work-up, the title compound **32** was obtained in 87% yield as white solid. ^{1}H NMR (400 MHz, DMSO-d_6) δ 8.84 (s, 1H), 8.68 (s, 1H), 8.41 (s, 1H), 8.26 (t, J = 5.6 Hz, 1H), 7.83 (d, J = 9.2 Hz, 1H), 7.71 (dd, J = 2.0, 1.6 Hz, 1H), 7.47 (d, J = 12.4 Hz, 1H), 7.38 (d, J = 8.6 Hz, 2H), 7.32–7.22 (m, 2H), 7.19 (d, J = 8.6 Hz, 2H), 7.00 (ddd, J = 7.6, 2.4, 2.0 Hz, 1H), 4.21 (q, J = 6.8 Hz, 2H), 3.72 (td, J = 7.6, 5.6 Hz, 2H), 2.91 (t, J = 7.6 Hz, 2H), 1.43 (t, J = 6.8 Hz, 3H). ^{13}C NMR (100 MHz, DMSO-d_6) δ 158.4, 155.3 (d, $J_{C\text{-}F}$ = 251.7 Hz), 154.2, 152.4, 145.7 (d, $J_{C\text{-}F}$ = 12.4 Hz), 144.8 (d, $J_{C\text{-}F}$ = 12.1 Hz), 141.4, 137.6, 133.3, 133.2, 130.4, 129.1, 121.4, 118.6, 117.5, 116.6, 112.5 (d, $J_{C\text{-}F}$ = 17.3 Hz), 111.9, 105.4, 64.9, 42.4, 34.1, 14.4. LC-MS (ESI) m/z: 480.2 $[M+H]^+$. HRMS (ESI) m/z: calcd for $C_{25}H_{24}ClFN_5O_2$, 480.1603 $[M+H]^+$, found 480.1601. HPLC purity: 98.3%, t_R = 19.37 min.

1-(4-{2-[(7-Ethoxy-6-fluoroquinazolin-4-yl*)amino]ethyl}phenyl)-3-phenylurea (**33**).* The title compound was synthesized following the general procedure B and using the reactants/reagents **19d** (98 mg, 0.30 mmol, 1.0 equiv.), isocyanatobenzene (55 mg, 0.46 mmol, 1.5 equiv.), methanol (0.09 mL) and dichloromethane (9 mL). After stirred for 2 h at room temperature and work-up, the title compound **33** was obtained in 97% yield as white solid. ^{1}H NMR (400 MHz, DMSO-d_6) δ 8.61 (s, 1H), 8.58 (s, 1H), 8.43 (s, 1H), 8.13–8.04 (m, 2H), 7.44 (dd, J = 8.8, 1.4 Hz, 2H), 7.37 (d, J = 8.4 Hz, 2H), 7.30–7.23 (m, 3H), 7.17 (d, J = 8.4 Hz, 2H), 6.95 (tt, J = 7.6, 1.2 Hz, 1H), 4.24 (q, J = 7.2 Hz, 2H), 3.70 (td, J = 7.8, 6.4 Hz, 2H), 2.88 (t, J = 7.8 Hz, 2H), 1.41 (t, J = 7.2 Hz, 3H). ^{13}C NMR (100 MHz, DMSO-d_6) δ 158.8 (d, $J_{C\text{-}F}$ = 3.8 Hz), 155.1, 152.6, 151.1 (d, $J_{C\text{-}F}$ = 12.9 Hz), 150.2 (d, $J_{C\text{-}F}$ = 245.2 Hz), 147.9, 139.8, 137.8, 132.9, 129.0, 128.8, 121.8, 118.4, 118.2, 109.7, 108.0 (d, $J_{C\text{-}F}$ = 6.5 Hz), 107.8 (d, $J_{C\text{-}F}$ = 20.1 Hz), 64.6, 42.3, 34.0, 14.3. LC-MS (ESI) m/z: 446.2 $[M+H]^+$. HRMS (ESI) m/z: calcd for $C_{25}H_{25}FN_5O_2$, 446.1992 $[M+H]^+$, found 446.1986. HPLC purity: 99.4%, t_R = 17.08 min.

1-(4-{2-[(7-Ethoxy-6-fluoroquinazolin-4-yl*)amino]ethyl}phenyl)-3-(3-fluorophenyl)urea (**34**).* The title compound was synthesized following the general procedure B and using the reactants/reagents **19d** (98 mg, 0.30 mmol, 1.0 equiv.), 1-fluoro-3-isocyanatobenzene (60 mg, 0.44 mmol, 1.5 equiv.), methanol (0.09 mL) and dichloromethane (9 mL). After stirred for 2 h at room temperature and work-up, the title compound **34** was obtained in 84% yield as white solid. ^{1}H NMR (400 MHz, DMSO-d_6) δ 8.87 (s, 1H), 8.67 (s, 1H), 8.43 (s, 1H), 8.16–8.02 (m, 2H), 7.48 (ddd, J = 12.0, 2.6, 2.2 Hz, 1H), 7.37 (d, J = 8.4 Hz, 1H), 7.34–7.22 (m, 2H), 7.18 (d, J = 8.4 Hz, 2H), 7.10 (ddd, J = 8.4, 2.2, 2.2 Hz, 1H), 6.77 (dddd, J = 8.8, 8.4, 2.6, 2.2 Hz, 1H), 4.24 (q, J = 7.0 Hz, 2H), 3.70 (td, J = 8.0, 6.0 Hz, 2H), 2.88 (t, J = 8.0 Hz, 2H), 1.41 (t, J = 7.0 Hz, 3H). ^{13}C NMR (100 MHz, DMSO-d_6) δ 162.5 (d, $J_{C\text{-}F}$ = 239.6 Hz), 158.8, 155.1, 152.4, 151.1 (d, $J_{C\text{-}F}$ = 12.8 Hz), 150.2 (d, $J_{C\text{-}F}$ = 145.1 Hz), 147.9, 141.7 (d, $J_{C\text{-}F}$ = 11.5 Hz), 137.6, 133.2, 130.3 (d, $J_{C\text{-}F}$ = 9.7 Hz), 129.1, 118.6, 113.9, 109.7, 108.1 (d, $J_{C\text{-}F}$ = 21.6 Hz), 107.8 (d, $J_{C\text{-}F}$ = 23.7 Hz), 104.8 (d, $J_{C\text{-}F}$ = 25.9 Hz), 64.6, 42.3, 34.0, 14.3. LC-MS (ESI) m/z: 464.2 $[M+H]^+$. HRMS (ESI) m/z: calcd for $C_{25}H_{24}F_2N_5O_2$, 464.1898 $[M+H]^+$, found 464.1860. HPLC purity: 98.8%, t_R = 17.90 min.

1-(4-{2-[(7-Ethoxy-6-fluoroquinazolin-4-yl*)amino]ethyl}phenyl)-3-[3-(trifluoromethyl)phenyl]urea (**35**).* The title compound was synthesized following the general procedure B and using the reactants/reagents **19d** (196 mg, 0.60 mmol, 1.0 equiv.), 1-isocyanato-3-(trifluoromethyl)benzene (163 mg, 0.87 mmol, 1.5 equiv.), methanol (0.2 mL) and dichloromethane (20 mL). After work-up, the title compound **35** was obtained in 89% yield as white solid. ^{1}H NMR (400 MHz, DMSO-d_6) δ 9.03 (s, 1H), 8.75 (s, 1H), 8.43 (s, 1H), 8.16–7.98 (m, 3H), 7.56 (d, J = 8.0 Hz, 1H) 7.50 (dd, J = 8.0, 7.6 Hz, 2H), 7.39 (d, J = 8.4 Hz, 2H), 7.30 (d, J = 7.2 Hz, 1H), 7.26 (d, J = 8.4 Hz, 1H), 7.18 (d, J = 8.4 Hz, 2H), 4.24 (q, J = 7.0 Hz, 2H), 3.70 (td, J = 7.2, 6.0 Hz, 2H), 2.89 (t, J = 7.2 Hz, 2H), 1.41 (t, J = 7.0 Hz, 3H). ^{13}C NMR (150 MHz, DMSO-d_6) δ 158.7, 155.1, 152.5, 151.1 (d, $J_{C\text{-}F}$ = 12.9 Hz), 150.1 (d, $J_{C\text{-}F}$ = 245.4 Hz), 147.8, 140.7, 137.5, 133.3, 129.8, 129.5 (q, $J_{C\text{-}F}$ = 31.4 Hz), 129.0, 124.2 (q, $J_{C\text{-}F}$ = 270.6 Hz), 121.7, 118.6, 117.9, 114.0, 109.7, 108.0 (d, $J_{C\text{-}F}$ = 5.7 Hz), 107.8 (d, $J_{C\text{-}F}$ = 20.0 Hz), 64.5, 42.2, 33.9, 14.3. LC-MS (ESI) m/z: 514.3 $[M+H]^+$. HRMS (ESI) m/z: calcd for $C_{26}H_{24}F_4N_5O_2$, 514.1866 $[M+H]^+$, found 514.1863. HPLC purity: 98.6%, t_R = 19.61 min.

1-(3-Chloro-4-fluorophenyl)-3-(4-{2-[(7-ethoxy-6-fluoroquinazolin-4-yl*)amino]ethyl}phenyl)urea (**36**).* The title compound was synthesized following the general procedure B and using the reactants/reagents **19d** (40 mg, 0.12 mmol, 1.0 equiv.), 2-chloro-1-fluoro-4-isocyanatobenzene (81 mg, 0.30 mmol, 2.5 equiv.), methanol (0.2 mL) and dichloromethane (2 mL). After work-up, the title compound **36** was obtained in 73% yield as white

solid. ^{1}H NMR (400 MHz, DMSO-d_6) δ 8.83 (s, 1H), 8.68 (s, 1H), 8.42 (s, 1H), 8.13–8.04 (m, 2H), 7.79 (dd, J = 4.8, 2.4 Hz, 1H) 7.37 (d, J = 8.4 Hz, 2H), 7.34–7.27 (m, 2H), 7.24 (d, J = 8.4 Hz, 1H), 7.17 (d, J = 8.4 Hz, 2H), 4.23 (q, J = 7.0 Hz, 2H), 3.69 (td, J = 7.6, 6.4 Hz, 2H), 2.88 (t, J = 7.6 Hz, 2H), 1.40 (t, J = 7.0 Hz, 3H). ^{13}C NMR (150 MHz, DMSO-d_6) δ 158.7 (d, $J_{C\text{-}F}$ = 3.5 Hz), 155.1, 152.3 (d, $J_{C\text{-}F}$ = 239.4 Hz), 152.2, 151.0 (d, $J_{C\text{-}F}$ = 12.9 Hz), 150.1 (d, $J_{C\text{-}F}$ = 245.3 Hz), 147.8, 137.5, 137.1 (d, $J_{C\text{-}F}$ = 2.1 Hz), 133.1, 129.0, 119.4, 119.1 (d, $J_{C\text{-}F}$ = 18.2 Hz), 118.6, 118.4 (d, $J_{C\text{-}F}$ = 6.5 Hz), 116.8 (d, $J_{C\text{-}F}$ = 21.6 Hz), 109.7, 108.0 (d, $J_{C\text{-}F}$ = 7.4 Hz), 107.7 (d, $J_{C\text{-}F}$ = 20.1 Hz), 64.5, 42.1, 33.9, 14.3. LC-MS (ESI) m/z 498.1 $[M+H]^+$. HRMS (ESI) m/z: calcd for $C_{25}H_{23}ClF_2N_5O_2$, 498.1508 $[M+H]^+$, found 498.1506. HPLC purity: 96.4% (t_R = 21.57 min).

*1-[4-Chloro-3-(trifluoromethyl)phenyl]-3-(4-{2-[(7-ethoxy-6-fluoroquinazolin-*4-yl*)amino]ethyl}phenyl)urea (**37**).* The title compound was synthesized following the general procedure B and using the reactants/reagents **19d** (40 mg, 0.12 mmol, 1.0 equiv.), 1-chloro-4-isocyanato-2-(trifluoromethyl)benzene (97 mg, 0.31 mmol, 2.5 equiv.), methanol (0.2 mL) and dichloromethane (2 mL). After work-up, the title compound **37** was obtained in 37% yield as white solid. ^{1}H NMR (400 MHz, DMSO-d_6) δ 9.15 (s, 1H), 8.79 (s, 1H), 8.42 (s, 1H), 8.14–8.02 (m, 3H), 7.62 (dd, J = 8.8, 2.4 Hz, 1H), 7.58 (d, J = 8.8 Hz, 1H), 7.38 (d, J = 8.4 Hz, 2H), 7.24 (d, J = 8.4 Hz, 1H), 7.18 (d, J = 8.4 Hz, 2H), 4.24 (q, J = 6.8 Hz, 2H), 3.69 (td, J = 7.4, 6.4 Hz, 2H), 2.89 (t, J = 7.4 Hz, 2H), 1.40 (t, J = 6.8 Hz, 3H). ^{13}C NMR (150 MHz, DMSO-d_6) δ 158.7 (d, $J_{C\text{-}F}$ = 3.0 Hz), 155.1, 152.4, 151.1 (d, $J_{C\text{-}F}$ = 12.8 Hz), 150.1 (d, $J_{C\text{-}F}$ = 245.2 Hz), 147.9, 139.4, 137.3, 133.4, 131.9, 129.0, 126.7 (q, $J_{C\text{-}F}$ = 30.3 Hz), 122.9, 122.8 (q, $J_{C\text{-}F}$ = 271.4 Hz), 122.1, 118.8, 116.6 (d, $J_{C\text{-}F}$ = 5.4 Hz), 109.7, 108.0 (d, $J_{C\text{-}F}$ = 7.1 Hz), 107.7 (d, $J_{C\text{-}F}$ = 20.0 Hz), 64.5, 42.2, 33.9, 14.3. LC-MS (ESI) m/z: 548.1 $[M+H]^+$. HRMS (ESI) m/z: calcd for $C_{26}H_{23}ClF_4N_5O_2$, 548.1476 $[M+H]^+$, found 548.1454. HPLC purity: 98.1% (t_R = 24.11 min).

*1-(5-Chloro-2-methoxyphenyl)-3-(4-{2-[(7-ethoxy-6-fluoroquinazolin-*4-yl*)amino]ethyl}phenyl)urea (**38**).* The title compound was synthesized following the general procedure B and using the reactants/reagents **19d** (82 mg, 0.25 mmol, 1.0 equiv.), 4-chloro-2-isocyanato-1-methoxybenzene (69 mg, 0.38 mmol, 1.5 equiv.), methanol (0.2 mL) and dichloromethane (2 mL). After stirred for 2 h at room temperature and work-up, the title compound **38** was obtained in 80% yield as white solid. ^{1}H NMR (400 MHz, DMSO-d_6) δ 9.34 (s, 1H), 8.43 (s, 1H), 8.37 (s, 1H), 8.23 (d, J = 2.6 Hz, 1H), 8.13–8.04 (m, 2H), 7.37 (d, J = 8.4 Hz, 2H), 7.25 (d, J = 8.4 Hz, 1H), 7.18 (d, J = 8.4 Hz, 2H), 7.02 (d, J = 8.8 Hz, 1H), 6.97 (dd, J = 8.8, 2.6 Hz, 1H), 4.24 (q, J = 7.0 Hz, 2H), 3.88 (s, 3H), 3.70 (td, J = 7.8, 6.4 Hz, 2H), 2.89 (t, J = 7.8 Hz, 2H), 1.41 (t, J = 7.0 Hz, 3H). ^{13}C NMR (100 MHz, DMSO-d_6) δ 158.7 (d, $J_{C\text{-}F}$ = 3.8 Hz), 155.1, 152.2, 151.0 (d, $J_{C\text{-}F}$ = 13.0 Hz), 150.1 (d, $J_{C\text{-}F}$ = 245.2 Hz), 147.9, 146.3, 137.6, 133.1, 130.1, 129.1, 124.4, 120.7, 118.2, 117.3, 111.8, 109.7, 108.0 (d, $J_{C\text{-}F}$ = 7.4 Hz), 107.8 (d, $J_{C\text{-}F}$ = 20.2 Hz), 64.5, 56.1, 42.2, 33.9, 14.3. LC-MS (ESI) m/z: 510.1 $[M+H]^+$. HRMS (ESI) m/z: calcd for $C_{26}H_{26}ClFN_5O_3$, 510.1708 $[M+H]^+$, found 510.1725. HPLC purity: 98.4%, t_R = 20.75 min.

*1-(4-{2-[(7-Ethoxy-6-fluoroquinazolin-*4-yl*)amino]ethyl}phenyl)-3-[2-methoxy-5-(trifluoromethyl)phenyl]urea (**39**).* The title compound was synthesized following the general procedure B and using the reactants/reagents **19d** (82 mg, 0.25 mmol, 1.0 equiv.), 2-isocyanato-1-methoxy-4-(trifluoromethyl)benzene (82 mg, 0.38 mmol, 1.5 equiv.), methanol (0.2 mL) and dichloromethane (2 mL). After stirred for 2 h at room temperature and work-up, the title compound **39** was obtained in 76% yield as white solid. ^{1}H NMR (400 MHz, DMSO-d_6) δ 9.38 (s, 1H), 8.55 (d, J = 2.4 Hz, 1H), 8.49 (s, 1H), 8.43 (s, 1H), 8.20–8.02 (m, 2H), 7.39 (d, J = 8.4 Hz, 2H), 7.30 (dd, J = 8.8, 2.4 Hz, 1H), 7.25 (d, J = 8.4 Hz, 1H), 7.22–7.15 (m, 3H), 4.24 (q, J = 6.8 Hz, 2H), 3.96 (s, 3H), 3.70 (td, J = 7.2, 6.8 Hz, 2H), 2.89 (t, J = 7.2 Hz, 2H), 1.41 (t, J = 6.8 Hz, 3H). ^{13}C NMR (150 MHz, DMSO-d_6) δ 158.7 (d, $J_{C\text{-}F}$ = 3.0 Hz), 155.1, 152.4, 151.1 (d, $J_{C\text{-}F}$ = 12.9 Hz), 150.1 (d, $J_{C\text{-}F}$ = 245.3 Hz), 150.0, 147.9, 137.6, 133.2, 129.5, 129.1, 124.6 (q, $J_{C\text{-}F}$ = 269.6 Hz), 121.1 (q, $J_{C\text{-}F}$ = 31.5 Hz), 118.6 (q, $J_{C\text{-}F}$ = 3.0 Hz), 118.2, 114.0 (q, $J_{C\text{-}F}$ = 31.5 Hz), 110.7, 109.7, 108.0 (d, $J_{C\text{-}F}$ = 7.2 Hz), 107.8 (d, $J_{C\text{-}F}$ = 20.1 Hz), 64.5, 56.2, 42.2, 34.0, 14.3. LC-MS (ESI) m/z: 544.2 $[M+H]^+$. HRMS (ESI) m/z: calcd for $C_{27}H_{26}F_4N_5O_3$, 544.1972 $[M+H]^+$, found 544.1966. HPLC purity: 98.8%, t_R = 20.18 min.

*Docking Analysis of **BPR1K871** and Compound **23** with AURA and TRKA proteins.* The protein structures of AURA (PDB: 4JBO) and TRKA (PDB: 6PL1) were utilized for this study. The docking analysis was conducted using the Discovery Studio 2020//LigandFit program (BIOVIA Inc., San Diego, CA, USA) with the CHARMm force field [44]. The number of docking poses was set as 10 with default parameters. The decision of the best pose was according to the lowest binding energy of the compound as well as the nitrogen atom of the compound formed a hydrogen bond with the back bone amide nitrogen of Ala213 in AURA and Met592 in TRKA, respectively. This was imposed based on the observation of such both hydrogen bonds in the crystal structures of the AURA kinase complexed to **BPR1K871** (PDB: 4JBO), and in the crystal structures of the TRKA kinase complexed to entrectinib (PDB: 5KVT).

Purified Kinase Confirmatory Activity Assay for TRKA, AURA and AURB. The recombinant GST-TRKA (residues G443~G796, NP_002520.2) containing kinase domain (KD) expressed in Sf9 insect cells. The TRKA ADP-Kinase-Glo assay was carried out in 96-well plates at 30 °C for 180 min in a final volume of 10 μL including 200 ng GST-TRKA proteins, 25 mM Tris–HCl, pH 7.4, 2 mM DTT, 10 mM $MgCl_2$, 0.01% bovine serum albumin, 40 μM poly (Glu,Tyr) 4:1 peptide, 0.02% Triton X-100, 0.5 mM Na_3VO_4, and 40 μM ATP. Following incubation, 5 μL ADP-Glo™ Reagent (Promega, Madison, WI, USA) was added and the mixture was incubated at 25 °C for 40 min. The KDR (Kinase Detection Reagent) reagent 10 μL was added and the mixture was incubated 25 °C for 30 min. After incubation, 15 μL buffer (25 mM Tris-HCl, pH 7.4) was added and mixed well. Then 30 μL aliquot of each reaction mixture was transferred to 96-well black microtiter plate (237108, NUNC) and the luminescence was measured on Wallac Vector 1420 multi-label counter (PerkinElmer, Shelton, CT, USA). The AURKA ATP-Kinase-Glo and AURKB ATP-Kinase-Glo assays for the compounds were carried out as described in our previous studies [33,45].

Cellular Proliferation Assays. To determine cell viability after drug treatment, assays were performed by seeding 5000 KM12 cells per well in a 96-well culture plate. After 16 h, cells were then treated with vehicle or various concentrations of compound in medium for 72 h. The viable cells were quantitated using the MTS method (Promega, Madison, WI, USA) according to the manufacturer's recommended protocol. The results were determined by measuring the absorbance at 490 nm using a plate reader (Victor 2; PerkinElmer, Shelton, CT, USA). The IC_{50} value was defined as the amount of compound that caused 50% reduction in cell viability in comparison with DMSO-treated (vehicle) control and was calculated using Prism version 8 software (GraphPad, San Diego, CA, USA).

Western Blot Analysis. KM12 cells (1×10^6) were seeded in each well of a six-well plate for overnight in culture medium. After 40 min of compound treatment, cells were harvested by washing twice with cold PBS and lysed in RIPA buffer (20 mM Tris, pH 7.5, 150 mM NaCl, 1 mM Na_2EDTA, 1 mM EGTA, 1% NP-40, 1% sodium deoxycholate, 2.5 mM sodium pyrophosphate, 1 mM β-glycerophosphate, 1 mM Na_3VO_4, 1 μg/mL leupeptin, 1 mM PMSF, phosphatase inhibitor cocktail (Bimake, B15001), and protease inhibitor (Thermo Fisher, A32955). After addition of SDS sample buffer, the lysate was heated at 95 °C for 10 min and an amount of 50 μg of samples were resolved by SDS-PAGE and transferred onto a polyvinylidene difluoride (PVDF) membrane (Millipore, Bedford, MA,

USA). The membranes were immunoblotted with appropriate antibodies (TRKA Antibody (Cell Signaling Technology, #2505), Phospho-TrkA (Tyr490) Antibody (Cell Signaling Technology, #9141), and β-ACTIN antibody (Thermo Fisher, MA5-15739)) and detected using the SuperSignal reagent (Pierce, Rockford, IL, USA) followed by exposure to X-ray film.

Cell Culture. Human cancer cell line KM12 cells were cultured and maintained in flasks with RPMI-1640 Media. The culture medium was supplemented with 10% fetal bovine serum. The cells were incubated at 37 °C in a humidified atmosphere containing 5% CO_2.

Pharmacokinetics. Male ICR mice (25−35 g) and male Sprague Dawley rats (300−400 g) were obtained from BioLASCO (Taiwan Co., Ltd, Ilan, Taiwan). The animal studies were performed according to NHRI institutional animal care and committee-approved procedures. Rats were surgically prepared with a jugular-vein cannula 1 day before dosing. Rats and mice were fasted overnight (for approximately 18−20 h) before dosing. Water was available ad libitum throughout the experiment. Food was provided at 4 h after dosing. A single 2.0 and 10 mg/kg dose of compound, as a PEG400/DMA (80/20, v/v) for both IV and oral and DMSO/CrEL/D5W (5%/5%/90%,v/v/v) and 1%CMC+0.5%Tween 80 (oral) solution, was separately administered to rats and mice. The groups consisted of three rats each route and a total of 33 and 27 mice for intravenously (IV) and oral gavage (PO), respectively. Each rat received 2 or 10 mL of the dosing solution/kg of body weight and each mouse was given 100 and 200 μL of dosing solution by intravenous injection and by gavage, respectively. At 0 (before dosing), 2, 5 (IV only), 15, and 30 min and at 1, 2, 4, 6, 8, 16 (mice only), and 24 h after dosing, a blood sample (0.15 mL) was collected from each rat through the jugular-vein cannula and ~500 μL was collected from groups of three mice at each time point by cardiac puncture and stored in ice (0−4 °C). Immediately after collecting the blood sample, 150 mL of physiological saline (containing 30 Units of heparin per ml) was injected into the rat through the jugular-vein cannula. Plasma was separated from the blood by centrifugation (14,000 g for 15 min at 4 °C in a Beckman Model AllegraTM 6R centrifuge) and stored in a freezer (−80 °C). All samples were analyzed for the parent drug by LC−MS/MS. Data were acquired through selected reaction ion monitoring. Plasma concentration data were analyzed with a noncompartmental method.

Animal. The animal use protocol was approved by The Institutional Care and Use Committee of the National Health Research Institutes (animal use protocol number: NHRI-IACUC-106076-A). Briefly, Nude mice (*Nu-Fox 1*^{nu}) of six weeks old were purchased from BioLasco (Ilan, Taiwan) and housed in sterilized cages equipped with air filter and sterile beddings at the AAALAC accredited facility, Laboratory Animal Center of the National Health Research Institutes. Animals were fed standard mice chow with water available ad libitum. The animals were housed in group cages under a 12 h light/dark cycle.

In Vivo Antitumor Efficacy Studies in the KM12 Human Colorectal Cancer Xenograft Model (Subcutaneous inoculation of tumor cells in mice) KM12 cells were suspended in phenol red free RPMI-1640 medium and mixed with Matrigel™ (356237, BD Bioscience, San Jose CA, USA) in 1:1 ratio. The cells were subcutaneously inoculated into the left flanks of mice using a 1 mL syringe (needle 24G x 1 in., 0.25 mm; TERUMO). Cells were suspended in a volume so that 100 μL contains 1×10^6 KM12 cells per s. c. inoculation injection. The mice were randomly divided into 3 groups of 7−8 animals each, and the treatment was initiated. The animals will be grouped and treated with **39** at various doses for an optimal treatment period. Animals were treated with **39** at 100 mg/kg (P.O.) at day 1, 2, 3 after treatment, while the animal body weight loss<−10% on day 4. The dosage was reduced to 75 mg/kg and treated on day 4 and 5. After all this **39** group was treated at 75 mg/kg three time per week for 3 weeks. Vehicle (P.O.) 10 mL/kg QD for three continuous weeks the treatment schedule was 5 days on, 2 days off. Larotrectinib (**1**) at 75 mg/kg (P.O.), QD, the treatment schedule was 5 days on, 2 days off, and continued for 4 weeks. Tumor dimensions were measured with a digital caliper, and the tumor volume in mm^3 was calculated by the formula: Volume = (length x width^2)/2. Tumor-bearing mice were randomized when the mean tumor volume was approximately to 200 mm^3. All mice were monitored daily for signs of toxicity. Body weight and tumor size were measured twice a week.

Data Analysis and Statistics. Tumor growth inhibition (TGI) in percentage was determined by the formula: TGI (%) = (1-T/C) x 100, where T indicates the mean tumor volume of compound-treated group and C indicates the mean tumor volume of vehicle-treated control. The significant difference between drug treatment and vehicle control were performed with statistical analysis (p-value < 0.05 vs. control).

Declaration of competing interest

The authors declare that they have no known competing financial interests or personal relationships that could have appeared to influence the work reported in this paper.

Acknowledgement

Support from the National Health Research Institutes and Ministry of Science and Technology, Taiwan (MOST 109-2113-M-400-003 and MOST 109-3114-Y-001-001 for H.-P. H.) is acknowledged. This work is also financially supported by the Center of Applied Nanomedicine, National Cheng Kung University from The Featured Areas Research Center Program within the framework of the Higher Education Sprout Project by the Ministry of Education (MOE) in Taiwan. M.-C. L. is supported by the Ministry of Science and Technology, Taiwan (MOST 109-2113-M-400-003 and MOST 109-3114-Y-001-001), National Health Research Institutes, Taiwan, and Biomedical Translation Research Center, Academia Sinica, Taiwan. We thank Dr. Hsin-Ru Wu, Instruments Center at National Tsing Hua University, for her help in obtaining mass spectral data (MOST 110-2731-M-007-001) and Mr. Richard Guy for his help with English editing.

Appendix A. Supplementary data

Supplementary data to this article can be found online at https://doi.org/10.1016/j.ejmech.2021.113673.

Abbreviations

TRK	tropomyosin receptor kinase
NTRK	neurotrophic tyrosine receptor kinase
NT	neurotrophin
NGF	nerve growth factor
CRC	colorectal cancer
ETV6	ETS variant transcription factor 6
FDA	food and drug administration
DFG	Asp-Phe-Gly
MKI	multi-kinase inhibitor
IND	investigational new drug
AUR	aurora kinase
SAR	structure-activity relationship
FLT3	FMS-like tyrosine kinase 3
NRB	number of free rotatable bond
PSA	polar surface area

ATP	adenosine triphosphate
WT	wild-type
DDR1	discoidin domain receptor 1
PK	pharmacokinetic
AUC	area under curve
FOTO	five-days-on, two-days-off
TGI	tumor growth inhibition

References

[1] A. Nakagawara, Trk receptor tyrosine kinases: a bridge between cancer and neural development, Canc. Lett. 169 (2001) 107–114.
[2] E.J. Huang, L.F. Reichardt, TRK receptors: roles in neuronal signal transduction, Annu. Rev. Biochem. 72 (2003) 609–642.
[3] S.D. Skaper, The neurotrophin family of neurotrophic factors: an overview, Methods Mol. Biol. 846 (2012) 1–12.
[4] E. Cocco, M. Scaltriti, A. Drilon, NTRK fusion-positive cancers and TRK inhibitor therapy, Nat. Rev. Clin. Oncol. 15 (2018) 731–747.
[5] S. Pulciani, E. Santos, A.V. Lauver, L.K. Long, S.A. Aaronson, M. Barbacid, Oncogenes in solid human tumours, Nature 300 (1982) 539–542, https://doi.org/10.1038/300539a0.
[6] T.R. Geiger, J.-Y. Song, A. Rosado, D.S. Peeper, Functional characterization of human cancer-derived TRKB mutations, PloS One 6 (2011), e16871.
[7] C. Miranda, M. Mazzoni, M. Sensi, M.A. Pierotti, A. Greco, Functional characterization of NTRK1 mutations identified in melanoma, Genes Chromosomes Cancer 53 (2014) 875–880.
[8] G.W. Reuther, Q.T. Lambert, M.A. Caligiuri, C.J. Der, Identification and characterization of an activating TrkA deletion mutation in acute myeloid leukemia, Mol. Cell Biol. 20 (2000) 8655–8666.
[9] M.H. Tomasson, Z. Xiang, R. Walgren, Y. Zhao, Y. Kasai, T. Miner, R.E. Ries, O. Lubman, D.H. Fremont, M.D. McLellan, J.E. Payton, P. Westervelt, J.F. DiPersio, D.C. Link, M.J. Walter, T.A. Graubert, M. Watson, J. Baty, S. Heath, W.D. Shannon, R. Nagarajan, C.D. Bloomfield, E.R. Mardis, R.K. Wilson, T.J. Ley, Somatic mutations and germline sequence variants in the expressed tyrosine kinase genes of patients with de novo acute myeloid leukemia, Blood 111 (2008) 4797–4808.
[10] C. Lagadec, S. Meignan, E. Adriaenssens, B. Foveau, E. Vanhecke, R. Romon, R.-A. Toillon, B. Oxombre, H. Hondermarck, X. Le Bourhis, TrkA overexpression enhances growth and metastasis of breast cancer cells, Oncogene 28 (2009) 1960–1970.
[11] A.M. Lange, H.-W. Lo, Inhibiting TRK proteins in clinical cancer therapy, Cancer 10 (2018) 105.
[12] J.B. Rubin, R.A. Segal, Growth, survival and migration: the Trk to cancer, Canc. Treat Res. 115 (2004) 1–18.
[13] A. Vaishnavi, A.T. Le, R.C. Doebele, TRKing down an old oncogene in a new era of targeted therapy, Canc. Discov. 5 (2015) 25–34.
[14] W. Yan, N.R. Lakkaniga, F. Carlomagno, M. Santoro, N.Q. McDonald, F. Lv, N. Gunaganti, B. Frett, H.Y. Li, Insights into current tropomyosin receptor kinase (TRK) inhibitors: development and clinical application, J. Med. Chem. 62 (2019) 1731–1760.
[15] M.-C. Li, H.-P. Hsieh, Tumor-agnostic inhibitors in oncology: a new phase for precision medicine, J. Chin. Chem. Soc. 67 (2020) 2216–2224.
[16] R.C. Doebele, L.E. Davis, A. Vaishnavi, A.T. Le, A. Estrada-Bernal, S. Keysar, A. Jimeno, M. Varella-Garcia, D.L. Aisner, Y. Li, J. Stephens, D. Morosini, B.B. Tuch, M. Fernandes, N. Nanda, J.A. Low, An oncogenic NTRK fusion in a patient with soft-tissue sarcoma with response to the tropomyosin-related kinase inhibitor LOXO-101, Canc. Discov. 5 (2015) 1049–1057.
[17] M. Menichincheri, E. Ardini, P. Magnaghi, N. Avanzi, P. Banfi, R. Bossi, L. Buffa, G. Canevari, L. Ceriani, M. Colombo, L. Corti, D. Donati, M. Fasolini, E. Felder, C. Fiorelli, F. Fiorentini, A. Galvani, A. Isacchi, A.L. Borgia, C. Marchionni, M. Nesi, C. Orrenius, A. Panzeri, E. Pesenti, L. Rusconi, M.B. Saccardo, E. Vanotti, E. Perrone, P. Orsini, Discovery of entrectinib: a new 3-aminoindazole as a potent anaplastic lymphoma kinase (ALK), c-ros oncogene 1 kinase (ROS1), and pan-tropomyosin receptor kinases (Pan-TRKs) inhibitor, J. Med. Chem. 59 (2016) 3392–3408.
[18] C. Albanese, R. Alzani, N. Amboldi, N. Avanzi, D. Ballinari, M.G. Brasca, C. Festuccia, F. Fiorentini, G. Locatelli, W. Pastori, V. Patton, F. Roletto, F. Colotta, A. Galvani, A. Isacchi, J. Moll, E. Pesenti, C. Mercurio, M. Ciomei, Dual targeting of CDK and tropomyosin receptor kinase families by the oral inhibitor PHA-848125, an agent with broad-spectrum antitumor efficacy, Mol. Canc. Therapeut. 9 (2010) 2243–2254.
[19] J. Sachdev, H.T. Arkenau, J.R. Infante, M.M. Mita, S.P. Anthony, R.B. Natale, S. Ejadi, K. Wilcoxen, V. Kansra, H. Laken, L. Hughes, R. Martell, G.J. Weiss, 506 Phase (Ph) 1/2a study of TSR-011, a potent inhibitor of ALK and TRK, in advanced solid tumors including crizotinib-resistant ALK positive non-small cell lung cancer, Eur. J. Canc. 50 (2014) 165.
[20] P. Albaugh, Y. Fan, Y. Mi, F. Sun, F. Adrian, N. Li, Y. Jia, Y. Sarkisova, A. Kreusch, T. Hood, M. Lu, G. Liu, S. Huang, Z. Liu, J. Loren, T. Tuntland, D.S. Karanewsky, H.M. Seidel, V. Molteni, Discovery of GNF-5837, a selective TRK inhibitor with efficacy in rodent cancer tumor models, ACS Med. Chem. Lett. 3 (2012) 140–145.
[21] F.M. Yakes, J. Chen, J. Tan, K. Yamaguchi, Y. Shi, P. Yu, F. Qian, F. Chu, F. Bentzien, B. Cancilla, J. Orf, A. You, A.D. Laird, S. Engst, L. Lee, J. Lesch, Y.C. Chou, A.H. Joly, Cabozantinib (XL184), a novel MET and VEGFR2 inhibitor, simultaneously suppresses metastasis, angiogenesis, and tumor growth, Mol. Canc. Therapeut. 10 (2011) 2298–2308.
[22] P.P. Patwardhan, K.S. Ivy, E. Musi, E. de Stanchina, G.K. Schwartz, Significant blockade of multiple receptor tyrosine kinases by MGCD516 (Sitravatinib), a novel small molecule inhibitor, shows potent anti-tumor activity in preclinical models of sarcoma, Oncotarget 7 (2016) 4093–4109.
[23] J.J. Bailey, R. Schirrmacher, K. Farrell, V. Bernard-Gauthier, Tropomyosin receptor kinase inhibitors: an updated patent review for 2010-2016 – Part I, Expert Opin. Ther. Pat. 27 (2017) 733–751.
[24] J.J. Bailey, R. Schirrmacher, K. Farrell, V. Bernard-Gauthier, Tropomyosin receptor kinase inhibitors: an updated patent review for 2010-2016 – Part II, Expert Opin. Ther. Pat. 27 (2017) 831–849.
[25] J.J. Bailey, C. Jaworski, D. Tung, C. W€angler, B. W€angler, R. Schirrmacher, Tropomyosin receptor kinase inhibitors: an updated patent review for 2016-2019, Expert Opin. Ther. Pat. 30 (2020) 325–339.
[26] A.R. Parikh, R.B. Corcoran, Fast-TRKing drug development for rare molecular targets, Canc. Discov. 7 (2017) 934–936.
[27] A. Drilon, T.W. Laetsch, S. Kummar, S.G. DuBois, U.N. Lassen, G.D. Demetri, M. Nathenson, R.C. Doebele, A.F. Farago, A.S. Pappo, B. Turpin, A. Dowlati, M.S. Brose, L. Mascarenhas, N. Federman, J. Berlin, W.S. El-Deiry, C. Baik, J. Deeken, V. Boni, R. Nagasubramanian, M. Taylor, E.R. Rudzinski, F. MericBernstam, D.P.S. Sohal, P.C. Ma, L.E. Raez, J.F. Hechtman, R. Benayed, M. Ladanyi, B.B. Tuch, K. Ebata, S. Cruickshank, N.C. Ku, M.C. Cox, D.S. Hawkins, D.S. Hong, D.M. Hyman, Efficacy of Larotrectinib in TRK fusion-positive cancers in adults and children, N. Engl. J. Med. 378 (2018) 731–739.
[28] M. Russo, S. Misale, G. Crisafulli, G. Corti, G. Rospo, L. Novara, B. Mussolin, A. Bartolini, G. Wei, N. Cam, R. Patel, S. Yan, R. Shoemaker, R. Wild, G. Li, G. Siravegna, L. Lazzari, N.F. Di, A. Bardelli, A.S. Bianchi, S. Siena, Acquired resistance to the TRK inhibitor entrectinib in colorectal cancer, Canc. Discov. 6 (2016) 36–44.
[29] A. Drilon, R. Nagasubramanian, J.F. Blake, N. Ku, B.B. Tuch, K. Ebata, S. Smith, V. Lauriault, G.R. Kolakowski, B.J. Brandhuber, P.D. Larsen, K.S. Bouhana, S.L. Winski, R. Hamor, W.I. Wu, A. Parker, T.H. Morales, F.X. Sullivan, W.E. DeWolf, L.A. Wollenberg, P.R. Gordon, D.N. Douglas-Lindsay, M. Scaltriti, R. Benayed, S. Raj, B. Hanusch, A.M. Schram, P. Jonsson, M.F. Berger, J.F. Hechtman, B.S. Taylor, S. Andrews, S.M. Rothenberg, D.M. Hyman, A next-generation TRK kinase inhibitor overcomes acquired resistance to prior TRK kinase inhibition in patients with TRK fusion-positive solid tumors, Canc. Discov. 7 (2017) 963–972.
[30] A. Drilon, S.I. Ou, B.C. Cho, D.W. Kim, J. Lee, J.J. Lin, V.W. Zhu, M.J. Ahn, D.R. Camidge, J. Nguyen, D. Zhai, W. Deng, Z. Huang, E. Rogers, J. Liu, J. Whitten, J.K. Lim, S. Stopatschinskaja, D.M. Hyman, R.C. Doebele, J.J. Cui, A.T. Shaw, Repotrectinib (TPX-0005) is a next-generation ROS1/TRK/ALK inhibitor that potently inhibits ROS1/TRK/ALK solvent- front mutations, Canc. Discov. 8 (2018) 1227–1236.
[31] E. Cocco, J.E. Lee, S. Kannan, A.M. Schram, H.H. Won, S. Shifman, A. Kulick, L. Baldino, E. Toska, A. Arruabarrena-Aristorena, S. Kittane, F. Wu, Y. Cai, S. Arena, B. Mussolin, R. Kannan, N. Vasan, A.N. Gorelick, M.F. Berger, O. Novoplansky, S. Jagadeeshan, Y. Liao, U. Rix, S. Misale, B.S. Taylor, A. Bardelli, J.F. Hechtman, D.M. Hyman, M. Elkabets, E. de Stanchina, C.S. Verma, A. Ventura, A. Drilon, M. Scaltriti, TRK xDFG mutations trigger a sensitivity switch from type I to II kinase inhibitors, Canc. Discov. 11 (2021) 126–141.
[32] R. Somwar, N.E. Hofmann, B. Smith, I. Odintsov, M. Vojnic, I. Linkov, A. Tam, I. Khodos, M.S. Mattar, E. de Stanchina, D. Flynn, M. Ladanyi, A. Drilon, U. Shinde, M.A. Davare, NTRK kinase domain mutations in cancer variably impact sensitivity to type I and type II inhibitors, Commun. Biol. 3 (2020) 776.
[33] Y. Chang Hsu, M.S. Coumar, W.-C. Wang, H.-Y. Shiao, Y.-Y. Ke, W.-H. Lin, C.-C. Kuo, C.-W. Chang, F.-M. Kuo, P.-Y. Chen, S.-Y. Wang, A.-S. Li, C.-H. Chen, P.-C. Kuo, C.-P. Chen, M.-H. Wu, C.-L. Huang, K.-J. Yen, Y.-I. Chang, J.T.-A. Hsu, C.-T. Chen, T.-K. Yeh, J.-S. Song, C. Shih, H.-P. Hsieh, Discovery of BPR1K871, a quinazoline based, multi-kinase inhibitor for the treatment of AML and solid tumors: rational design, synthesis, in vitro and in vivo evaluation, Oncotarget 7 (2016) 86239–86256.
[34] J.T. Metz, E.F. Johnson, N.B. Soni, P.J. Merta, L. Kifle, P. Hajduk, Navigating the kinome, Nat. Chem. Biol. 7 (2011) 200–202.
[35] G.S. Falchook, C.C. Bastida, R. Kurzrock, Aurora kinase inhibitors in oncology clinical trials: current state of the progress, Semin. Oncol. 42 (2015) 832–848.
[36] I. Choudary, P.M. Barr, J. Friedberg, Recent advances in the development of Aurora kinases inhibitors in hematological malignancies, Ther. Adv. Hematol. 6 (2015) 282–294.
[37] L.R.P. de Siqueira, P.A.T. de Moraes Gomes, L.P. de Lima Ferreira, M.J.B. de Melo Rego, A.C.L. Leite, Multi-target compounds acting in cancer progression: focus onthiosemicarbazone, thiazole and thiazolidinone analogues, Eur. J. Med. Chem. 170 (2019) 237–260.
[38] S.-Y. Lin, C.-F. Chang, M.S. Coumar, P.-Y. Chen, F.-M. Kuo, C.-H. Chen, M.-C. Li, W.-H. Lin, P.-C. Kuo, S.-Y. Wang, A.-S. Li, C.-Y. Lin, C.-M. Yang, T.-K. Yeh, J.-S. Song, J.T.-A. Hsu, H.-P. Hsieh, Drug-like property optimization: discovery of orally bioavailable quinazoline-based multi-targeted kinase inhibitors, Bioorg. Chem. 98 (2020) 103689.
[39] D.F. Veber, S.R. Johnson, H.-Y. Cheng, B.R. Smith, K.W. Ward, K.D. Kopple, Molecular properties that influence the oral bioavailability of drug candidates, J. Med. Chem. 45 (2002) 2615–2623.

[40] Y.-Y. Ke, H.-Y. Shiao, Y. Chang Hsu, C.-Y. Chu, W.-C. Wang, Y.-C. Lee, W.-H. Lin, C.-H. Chen, J.T.-A. Hsu, C.-W. Chang, C.-W. Lin, T.-K. Yeh, Y.-S. Chao, M.S. Coumar, H.-P. Hsieh, 3D-QSAR-assisted drug design: identification of a potent quinazoline-based aurora kinase inhibitor, ChemMedChem 8 (2013) 136–148.

[41] G. Subramanian, Y. Zhu, S.J. Bowen, N. Roush, J.A. White, D. Huczek, T. Zachary, C. Javens, T. Williams, A. Janssen, A. Gonzales, Lead identification and characterization of *h*TrkA type 2 inhibitors, Bioorg, Med. Chem. Lett. 29 (2019), 126680–126680.

[42] T. Anastassiadis, S.W. Deacon, K. Devarajan, H. Ma, J.R. Peterson, Comprehensive assay of kinase catalytic activity reveals features of kinase inhibitor selectivity, Nat. Biotechnol. 29 (2011) 1039–1045.

[43] Y.-Y. Ke, C.-P. Chang, W.-H. Lin, C.-H. Tsai, I.-C. Chiu, W.-P. Wang, P.-C. Wang, P.-Y. Chen, W.-H. Lin, C.-F. Chang, P.-C. Kuo, J.-S. Song, C. Shih, H.-P. Hsieh, Y.-H. Chi, Design and synthesis of BPR1K653 derivatives targeting the backing pocket of Aurora kinases for selective isoform inhibition, Eur. J. Med. Chem. 151 (2018) 533–545.

[44] G. Wu, D.H. Robertson, C.L. Brools III, M. Vieth, Detailed analysis of grid-based molecular docking: a case study of CDOCKER—a CHARMm-based MD docking algorithm, J. Comput. Chem. 24 (2003) 1549–1562.

[45] M.S. Coumar, J.-S. Wu, J.-S. Leou, U.-K. Tan, C.-Y. Chang, T.-Y. Chang, W.-H. Lin, J.T.-A. Hsu, Y.-S. Chao, S.-Y. Wu, H.-P. Hsieh, Aurora kinase A inhibitors: identification, SAR exploration and molecular modeling of 6,7-dihydro-4*H*-pyrazolo[1,5-*a*]pyrrolo[3,4-*d*]pyrimidine-5,8-dione scaffold, Bioorg. Med. Chem. Lett 18 (2008) 1623–1627.